

Additional thesis (CIE5050-09)

Master track: Water Management  
Specialisation: Hydrology

# An analysis of hydrological and geotechnical parameters of rotational landslides in pegmatite lithology in North Western Rwanda



B. J. Walraven  
4165438

Supervisor:  
Dr. T.A. Bogaard

November 19, 2018

## Acknowledgements

This additional thesis falls under a PhD research by Judith Uwihirwe at TU Delft with the topic of “*The effect of land use change on the hydrogeotechnical processes triggering landslides in North Western Rwanda*”. To set up the research site 7 weeks of fieldwork were carried out in Rwanda. I thoroughly enjoyed working on this project which is in large due to my supervisors.

Thom, thank you for having such a cool project ready for me the moment I walked into your office. It was a great experience to dive into the world of landslides and your enthusiasm for the matter is contagious. It was great having you there for fieldwork the first week. I think I have rarely learned so many new things in a week, and the off-topic talks were also a nice change of pace. I appreciated the freedom you gave me in the project, but were also always ready to help. Thank you for that.

Judith, your work ethic inspired me. Thank you for introducing me to fieldwork the way fieldwork is done in Rwanda and to many of your colleagues so I could quickly stand on my feet there. And also, many thanks for the hospitality there and letting me be a temporary part of the household.

## Table of contents

Acknowledgements .....	1
Abstract .....	3
1. Introduction.....	4
2. Theory.....	5
2.1 Slope stability .....	5
2.2 Causes and triggers .....	6
3. Site description.....	7
3.1 Climate, topography, and geology .....	7
3.2 The sites.....	7
4. Methodology .....	10
4.1 Fieldwork .....	10
4.2 Lab analysis.....	12
5. Results .....	14
5.1 Ground water level and rainfall.....	14
5.2 Soil moisture tubes.....	15
5.3 Soil characteristics.....	16
5.4 Soil texture .....	19
6. Back analysis of slope stability .....	22
7. Discussion .....	24
8. Conclusion .....	26
Bibliography.....	27
Appendices .....	29
Appendix A – Additional piezometer data from Karago landslide .....	29
Appendix B – schematic of groundwater level in piezometers on slope M and S1 .....	30
Appendix C - Hydraulic conductivity and infiltration calculations .....	31
Appendix D – Unified Soil Classification System (from De Smedt (2013)) .....	33
Appendix E – Atterberg limits results for Karago landslide.....	34
Appendix F – Screenshots of SLIP5EX spreadsheet.....	35
Appendix G – Literature values for C and $\phi$ , and typical bulk unit weight for different soil types...	36
Appendix H – Landslide catalogue .....	37
Appendix I – Direct shear results moved slope M (layer 5) .....	40

## Abstract

Worldwide landslides cause a great amount of damage, as is also the case in Rwanda. Here more and more slopes fail as anthropogenic activities such as building, farming, or deforestation, are moved to marginal lands such as hillslopes. To investigate the hydrological response of typical hillslopes in North Western Rwanda five landslides are chosen from a previously set up landslide inventory of the region. These five landslides form the basis of a regional assessment for which geotechnical parameters like soil texture, cohesion, and angle of internal friction, are analysed. For one of the five also hydrological data is gathered. This data consists of soil moisture content, groundwater level, hydraulic conductivity, and infiltration for both the moved and the stable parts of the slope. With all this data a back analysis is performed to gather why the slope failed.

The soil texture results show that most of the soil layers investigated are sandy soil, with a slight fraction of clay. This is supported by the values for hydraulic conductivity and infiltration, and by the results of the back analysis, which is coherent with literature values. The direct shear results, however, yield quite high cohesion values, typical for clay, and high angle of internal friction values (even too high for sand sometimes). Thus, the soils can be classified as sand, but the influence of the fines is significant. The slope failure can be a result of a very thin weak soil layer, or anomaly in the soil skeleton, but this is difficult to represent in the tests carried out, with such small samples. Another reason for slope failure does not have to be internal but can be external, such as anthropogenic activities, or toe erosion by a river. It is therefore important to analyse the surroundings of the failed slope carefully.

It is wishful to extend hydrological measurements to more landslides and also wait longer to be able to gain more insight into the relation between precipitation, infiltration and groundwater levels, and the hillslope's hydrological response.

## 1. Introduction

Landslides are the most destructive natural hazard causing the highest social or economic damage to their environment (Reichenbach et al., 1998; Brabb, 1991). Though a single slope failure may be very local, and not as devastating as an earthquake or a flood, it occurs more frequently and abundantly than any other natural hazard. Often the damage caused by an earthquake or heavy storm is also (in)directly due to a subsequently triggered landslide (Varnes, 1984). Seen over longer periods of time this makes landslides cause more loss than any other hazard.

In Rwanda, as in most of sub-Saharan Africa, population density is increasing very fast (Clay & Lewis, 2003). This growing population pressure leads to deforestation and pushes agricultural activities to marginal lands such as hillslopes. In some cases, it has even led to people moving to hillslopes for housing (Van der Esch, 2003). The occupation of hillslopes for agricultural activities consequently leads to large scale soil and slope degradation. Land management practices such as terracing or (improper) irrigation have led to hillslope disturbance making it less stable (Knapen et al., 2006; Clay & Lewis, 2003).

Anthropogenic activities, such as building, forest cutting, or farming, can cause changes in the hydrogeotechnical properties of the hillslopes, such as groundwater level, infiltration capacity, and shear strength parameters. Considering that hillslopes are morphologically active landscapes and strongly affected by changes in land use, which affect hydrological and geotechnical behaviour, has brought those exploiting the hillslopes in a dangerous position. In recent years many landslides have occurred in Rwanda with abundant fatalities (Nsengiyumva, 2012). Despite government regulations to limit the occupation and land use change of the fragile hill slopes people still move there because they are driven more strongly by the socio-economic pressures (Clay & Lewis, 2003).

Through a better understanding of hydrogeotechnical behaviour of hillslopes, landslide events can be reduced, future damage caused by these landslides can be restricted, and appropriate land management techniques can be initiated. Therefore, this report aims to make a preliminary assessment of the causes and triggers of a selected number of slope failures in North Western Rwanda by first answering the research question:

*“What are the hydrogeotechnical characteristics of the selected landslides?”*

Five landslides in the North West region are chosen for the collection of geotechnical data. These five are the first in a landslide catalogue of the region aimed at getting ‘representative’ soil parameters to be able to assess the relation between hydrogeotechnical characteristics and slope failure. One of the five sites, with both a stable and a failed slope, will serve to collect both hydrological and geotechnical data. To this end, the second research question to be investigated here is:

*“What is the hydrological response of typical hillslopes in the North Western Rwanda?”*

## 2. Theory

### 2.1 Slope stability

A slope can start to move if the driving force is higher than the stabilizing force. This can be a result of either a decrease in frictional force, or an increase in the gravitational force (Bogaard, 2001).

A decrease in frictional force, or shear strength, can either be due to increase in pore water pressure or a decrease in material strength. An increase in pore water pressure in the soil skeleton causes a reduction in shear strength due to buoyancy forces exerted by the water on the soil if it is saturated, or a reduction in soil suction if the soil is unsaturated (Bogaard & Greco, 2015).

The principle of effective stress relates the total normal pressure to the pore water pressure in a soil through:

$$\sigma' = \sigma - u \quad (2.1)$$

$\sigma$  = total normal pressure [ $\text{kNm}^{-2}$ ]

$u$  = pore water pressure [ $\text{kNm}^{-2}$ ]

The deformations caused by the internal stress in the soil skeleton is almost completely determined by the changes of concentrated forces in the contact points between grains, and not the water surrounding the grains. Rolling and sliding of grains are what make the deformations visible. These shear stresses can be transmitted by the soil skeleton only. Therefore, a higher pore water pressure reduces the contact points between grains and thus reduces the shear strength of the soil (Verruijt, 2007).

An increase in gravitational shear stress can be induced by changes in slope geometry, such as undercutting or erosion, vibrations, such as earthquakes, and changes in surcharges, like vegetation or buildings (Bogaard, 2001).

According to Coulomb the shear stress  $\tau$  can be approximated by:

$$\tau = c + \sigma' \tan(\varphi) \quad (2.2)$$

Where:

$c$  = cohesion [ $\text{kPa}$ ]

$\varphi$  = angle of internal friction [ $^\circ$ ]

$\sigma'$  = effective normal stress [ $\text{kNm}^{-2}$ ]

The cohesion and angle of internal friction here are both material properties and the effective normal stress is related to the pore water pressure as seen before.

The stability of a slope is determined by the ratio between the strength (shear strength) and the load (shear force) along a surface of failure, the slip surface. This ratio is called the safety factor,  $F$ . For a basic circular slip surface this can be written as:

$$F = \frac{\sum[(c + \sigma' \tan \varphi) / \cos \alpha]}{\sum \gamma h \sin \alpha} \quad (2.3)$$

Where  $h$  is the height of a slice as shown in figure 2.1 and  $\gamma$  is the volumetric weight of the soil in the slice (Verruijt, 2007). The force acting on the potential soil sliding mass “is calculated as the integral of normal and shear stress along the boundary surface and summed to the weight of the mass” (Bogaard & Greco, 2015). The stability is assessed by applying the principle of moment with respect to the centre of the circle. It is assumed that if  $F > 1$  the slope is stable, and if  $F < 1$  it is not.

There are many different alterations proposed to formula (2.3). Fellenius assumed no forces between the adjacent slices, whereas Bishop did, but assumed the resultant force to be horizontal (Verruijt,

2007). Another form is the infinite slope hypothesis that assumes “the failure surface to be a plane parallel to the surface slope, reducing the factor of safety to the ratio of the limit shear stress to the actual shear stress parallel to the slope surface” (Bogaard & Greco, 2015). For data analysis in this report the program SLIP5EX is used, which is based on Fellenius and the infinite slope.

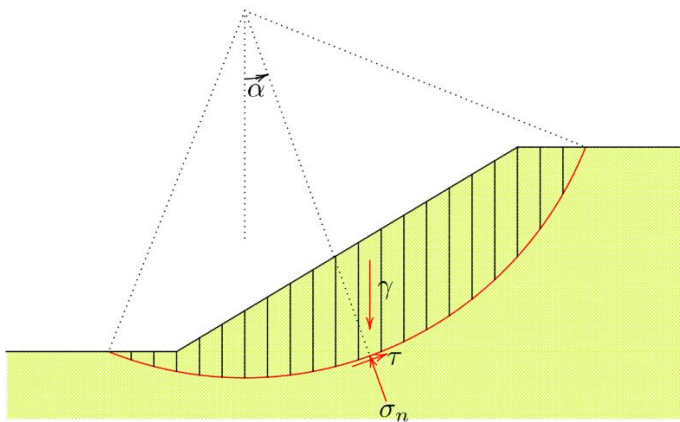


Figure 2.1: Circular slip surface. Basic assumption of most slope stability models (Verruijt, 2007)

## 2.2 Causes and triggers

A landslide occurring is more an exception than a rule, so when a slope fails something must have changed from the default situation. Underlying these changes in strength or load are certain causes and triggers. The difference between the two is in the time frame (Bogaard, 2001). What triggers a landslide is often a rapid development in stress conditions (an increase in gravity force), or in material strength (decrease in frictional force). The underlying causes, however, are usually a development over a longer period of time (Bogaard, 2001).

Though landslides can be triggered by a vast number of events such as earthquakes or excavations, the majority are triggered by (extreme) precipitation events (Malamud et al., 2004). Slope geomorphology and changes in land use are also factors that can cause landslides and may be subject to rapid change (Persichillo et al., 2016). Other predisposing factors for landslide occurrence are the geology, lithology, and soil structure of slopes, though these are fairly constant over long periods of time (Persichillo et al., 2016; Varnes, 1984).

Though it is known that water plays an important role in mass movement processes, the hydrological and geotechnical properties of the slopes and their surroundings studied in Rwanda, will have to be analysed carefully to find the actual reason of failure. Aside from causes and triggers landslides can also be classified by movement type (Varnes, 1978). In this study we limit ourselves to landslides of the rotational type, since that is the movement of the landslide of the main study site.



### 3. Site description

#### 3.1 Climate, topography, and geology

Rwanda is situated in the tropics (1°04'S - 2°51'S) but experiences a temperate climate due to its high elevation ranging from 970m amsl to 4507m amsl (Verdoodt & van Ranst, 2003). Most of the highlands and mountainous regions are found in the North West, with slopes between 8-40 degrees. Due to the higher elevation the North West also receives more rainfall and therefore has been the area with the most landslides and casualties in the past years (Nsengiyumva, 2012).

Rwanda knows two rainy seasons a year, one small one from September till November ( $\pm 430$  of the yearly 1300mm) and a larger one from March till May ( $\pm 480$  of the yearly 1300mm). The temperature is fairly stable around 20°C all year long.

The North Western part of Rwanda is partly located in the Congo-Nile divide. It is flanked to the North by the Virunga Mountains, and to the west by the Albertine Rift, also containing Lake Kivu. In this region the geology is made up of sedimentary, metamorphic and igneous rock. The predominant lithologies are schists, micaschists, pegmatites, granite, quartzite, and volcanic rocks (Verdoodt & van Ranst, 2003).

#### 3.2 The sites

From an existing landslide inventory made by J. Uwihirwe in the spring of 2018 five landslides were chosen for further study. The inventory contained extensive data on the location, geometry, land use, and possible cause of failure of nearly 600 landslides in the North Western region of Rwanda, specifically the Mukungwa river basin (Uwihirwe, 2018).

Five landslides in the North of the Western province of Rwanda were chosen for further study with the purpose of gaining more insight in the hydrogeotechnical behaviour of typical landslides in this region. For this regional assessment the selected landslides were all varying in size and land use (forestry, agriculture, or built-up), but they were all of the rotational type, and all on pegmatite lithology, one of the two main lithological units where most landslides occur (fig. 3.2). From these five landslides soil samples were taken for geotechnical analysis in the laboratory. More data on the landslides of this regional assessment can be found in Appendix H.

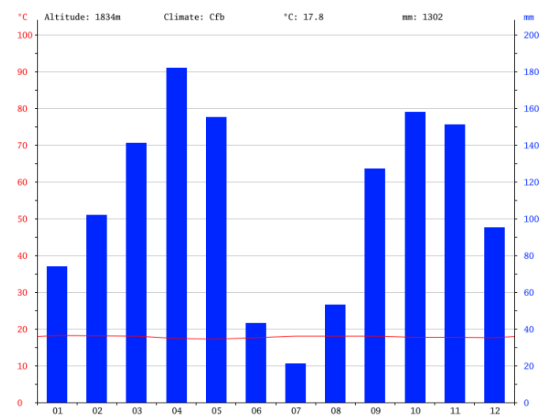


Figure 3.1: Yearly climate data chart of the Musanze district (N.W. Rwanda) ("Climate Musanze", 2018)



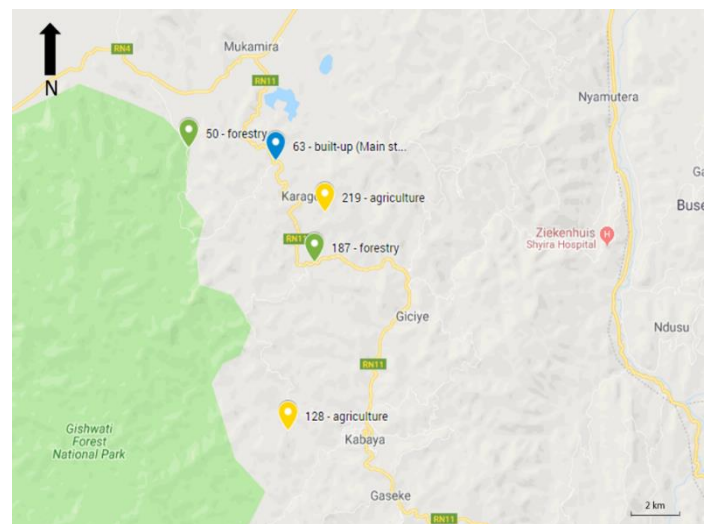


Figure 3.2: From top left to bottom right: 1) Landslide 50, 2) Main study site Karago landslide nr. 63, 3) Landslide 128, 4) Landslide 187, 5) Landslide 219, 6) Map of the area with all landslides, including land use, marked.



One of the five landslides, the Karago landslide nr. 63, was chosen for more detailed hydrological monitoring and became the main study site. It is located in the district of Nyabihu, Karago sector, Bukongora village ( $S1^{\circ}39'3.3$ ,  $E29^{\circ}30'30.7$ ). This landslide is situated just downslope of a paved road and used to have houses built at the edge of this road and some scattered forest on the slope, which later made place for agricultural land. The slope started to move in 2012 and failed completely in March 2016. Currently the houses surrounding the moved slope (fig. 3.3) are also showing signs of movement. The size of the landslide is approximately 60m long, 40m wide, and 8m deep. Adjacent to the moved slope is a stable ridge. At the bottom of the ridge there is a small open drain that drains excess water from the well to the river, and separates the stable ridge from another stable slope. The moved slope is vegetated by new crops. The stable ridge S0 contains mostly Eucalyptus coppices while slope S1 predominantly has full grown Eucalyptus, though these are both mixed with Eucalyptus of differing growth stages. Upslope (South) of the well there is a small agricultural plot.

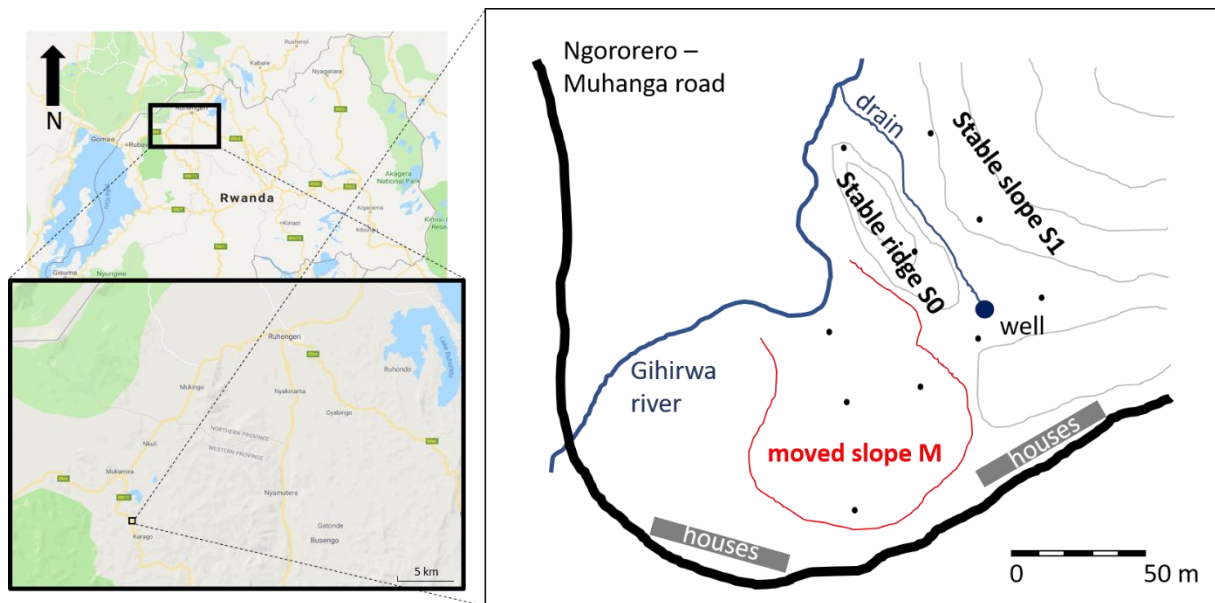


Figure 3.3: Schematic of the main study site, Karago landslide. The black dots represent piezometer installations.

## 4. Methodology

For the landslides nrs. 50, 128, 187, and 219 only sampling and subsequent geotechnical analysis in the laboratory was done. For the Karago landslide (nr. 63) hydrological and geotechnical analysis were both carried out. The geotechnical analysis consists of soil sampling in the field, followed by lab work to determine particle size distribution, bulk density, and shear strength of different soil layers. Hydrological analysis consists of measuring the groundwater level, soil moisture content, infiltration, and saturated permeability. In addition, a rain gauge was installed to monitor precipitation.

### 4.1 Fieldwork

#### *Groundwater and soil moisture*

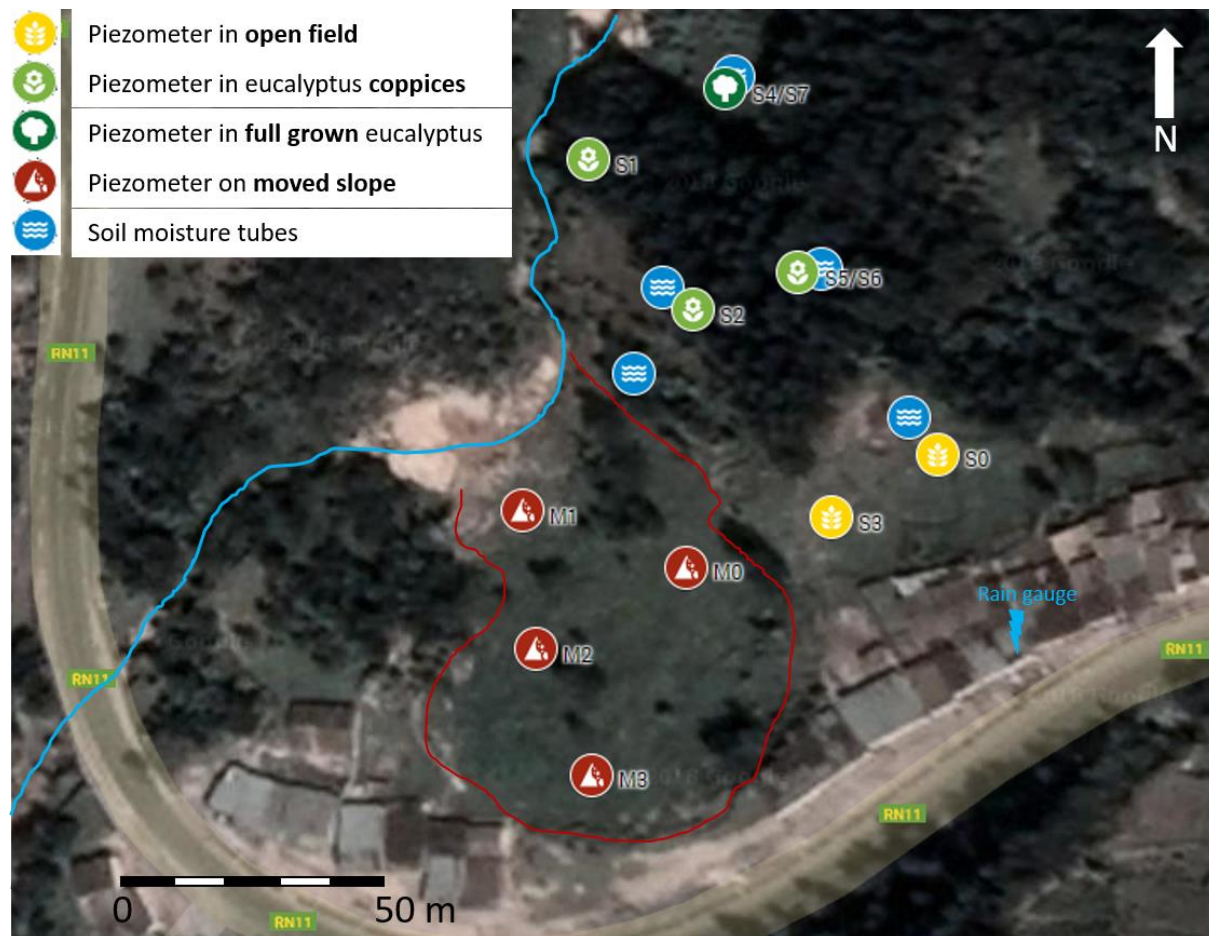


Figure 4.1: Location of piezometers installed at Karago landslide

At the Karago landslide piezometers were placed on both the moved and stable slope to measure the groundwater level. Four piezometers (M0, M1, M2, M3) were installed on the moved slope. Six piezometers were installed on stable slopes. Piezometers S1 and S2 were installed on a stable ridge with Eucalyptus coppices (0-9 months). Piezometers S5 and S6 were also installed in Eucalyptus coppices (<2 years). Piezometers S4 and S7 were installed in full grown Eucalyptus (>2 years). Piezometers S3 and S0 were installed upslope of the stable slope on small agricultural plots.

All the piezometers were self-made. PVC pipes ( $\varnothing$  5.5 cm) were placed in auger holes of diameter 7 or 10cm. The bottom  $\pm 40$ cm of the pipes were perforated and then covered with stockings to prevent soil from entering the pipe. After placement in the auger hole the remaining space was filled with sand to ensure free groundwater flow into the standpipes and prevent clogging. Additional piezometer data can be found in Appendix A.

Near a number of piezometers on the stable slopes, soil moisture access tubes for the Delta-T PR2 ("PR2 Profile Probe – analogue version", 2018) probe were installed (fig. 4.1). The maximum depth of these access tubes was 0.9 m.

In addition, an automatic logging rain gauge with a tipping bucket was installed on the rooftop of a house near the road (fig. 4.1).

#### *Saturated permeability and infiltration*

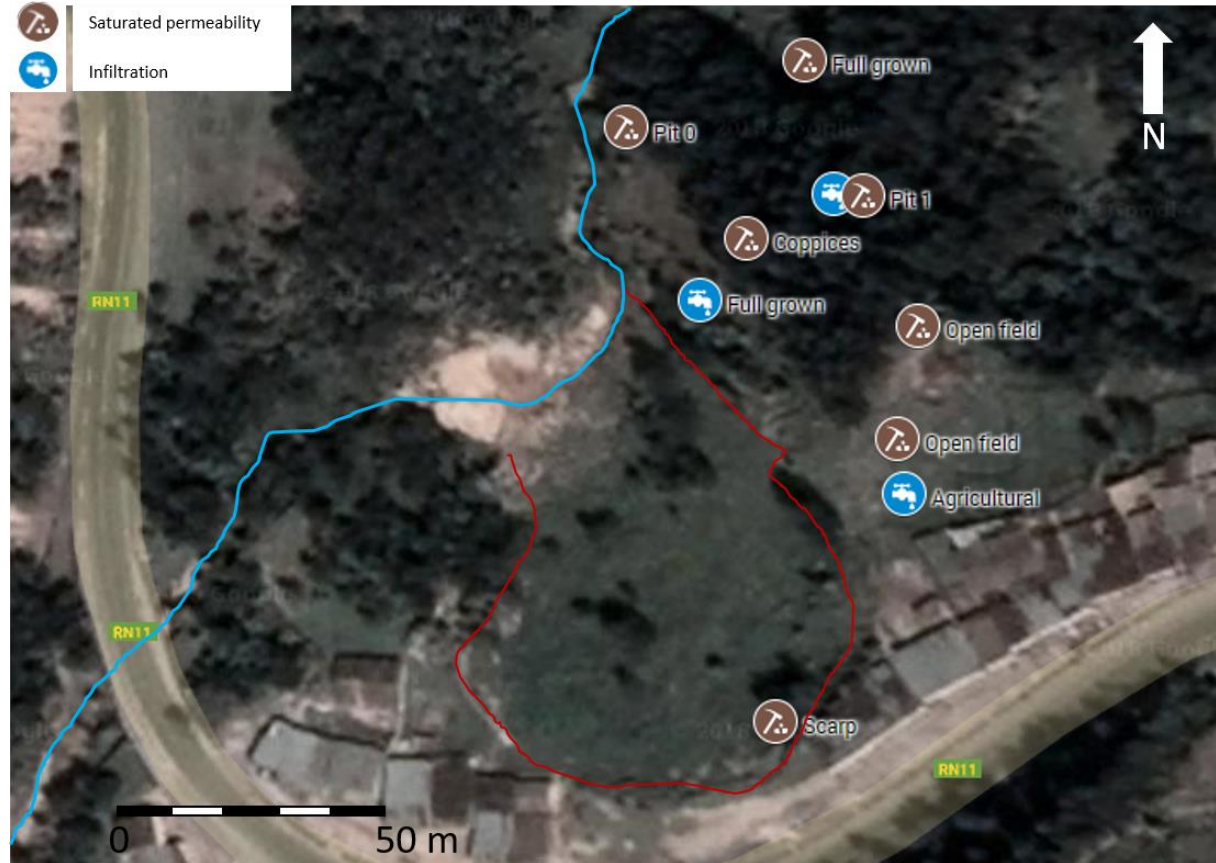


Figure 4.2: Location of double ring infiltrometer tests, and inverse auger hole tests and/or sampling location for constant head test

The saturated permeability was determined in-situ using the inverse auger hole method, because the soil layers considered were in the unsaturated zone. Inverse auger hole tests were carried out for as many soil layers as possible in the two pits dug on the stable slopes (fig. 4.2). In addition, several extra inverse auger hole tests were done in full grown Eucalyptus, Eucalyptus coppices, and in open field. The maximum depth of these tests was limited at 1.1m by the depth of the auger.

Following the Eco-Slopes Field Protocol from Cammeraat et al. (2001) for inverse auger hole tests (based on Kessler & Oosterbaan (1974)) a hole with diameter 7-10 cm was augered. The depth depended on the depth of the soil layers. If a layer was really thin (< 30cm) or augering a hole into the layer was too difficult due to large gravel stones, the layer was omitted. Otherwise  $\pm 35$ cm of water was thrown in and the drop of water level over time was measured manually or by using a pressure device ("TD-Diver", 2017) and translating the change in pressure to change in water depth. If time allowed the measurements were repeated once or twice.

For the infiltration tests a double ring infiltrometer with outer diameter 49.2cm and inner diameter 30cm, and ring heights of 84.2cm was used. The infiltration of the top soil layer near piezometers S2 (full grown Eucalyptus), S3 (agricultural plot) and near S5/S6 (Eucalyptus coppices) was measured in this way.



### Sampling

Soil sampling was done for particle size analysis, bulk density analysis, constant head testing, and direct shear testing. For particle size analysis a disturbed sample suffices. For bulk density, constant head, and direct shear testing and undisturbed sample is required. Undisturbed samples of the landslides 50, 128, 187, 219, and of the moved slope of the Karago landslide were taken from their scarps. To retrieve undisturbed samples from all layers from the stable slopes S0 and S1 at Karago two pits were dug (fig. 4.3). At each location the in-situ moisture content was also measured using the Delta-T ML3 soil moisture sensor ("ML3 ThetaProbe Soil Moisture Sensor", 2018).



Figure 4.3: Sampling pit 0 (on stable slope S0) left and sampling pit 1 (on stable slope S1) right

## 4.2 Lab analysis

### Lab Analysis

Particle size analysis was carried out using a dry sieving method for particles  $> 75\mu\text{m}$ . 13 sieves ranging from 4.75mm to 0.075mm were used. Particles smaller than  $75\mu\text{m}$  were analysed by sedimentation through a hydrometer test according to the standard test method for particle size analysis of soils from the ASTM (1998).

Following the core method as described in the Eco-Slopes Field Protocol (Cammeraat et al., 2001) the dry bulk density and the gravimetric soil moisture content were determined based on the loss of water from a sample dried for 24hrs at  $105^{\circ}\text{C}$ .

The saturated permeability was also tested in the laboratory using a self-made constant head test whereby a constant head is maintained across the soil sample to create a steady discharge through the sample. By attaching a core cylinder watertight on top of a sample container, and connecting that core cylinder watertight to a Mariotte bottle using a flexible tube, a constant head is maintained above the sample (fig. 4.4). The sample is covered at the bottom with gauze to prevent soil from flushing out, and raised slightly from the bottom to ensure free outflow of water.

For direct shear testing two different set ups were used. Though the procedure was the same, following the ISO/TS 17892-10 for consolidated drained tests, due to a change in location parts of the test were carried out with a square shearbox of  $36\text{cm}^2$  with drainage plates, and for the other tests a circular shearbox of  $31\text{cm}^2$  was used with porous plates. The shearing samples were removed from their original container undisturbed and reconsolidated, after which the samples were saturated from the bottom up. If a shearing sample failed to be removed undisturbed the sample ring would be filled with loose material and consolidated manually. This was especially the case for loose gravel or sandy soils. Tests were carried out consolidated drained at speeds of 1-3 mm/hr depending on the permeability of the sample.



*Figure 4.4: Saturated permeability set-up in laboratory (left) and close-up of sample being tested (right)*

## 5. Results

This chapter aims to answer the question ‘*what are the hydrogeotechnical characteristics of the mapped landslides?*’. Data from the fieldwork at the main study site, Karago landslide nr. 63, is presented here. Further analysis of the data is discussed in subsequent chapters.

### 5.1 Ground water level and rainfall

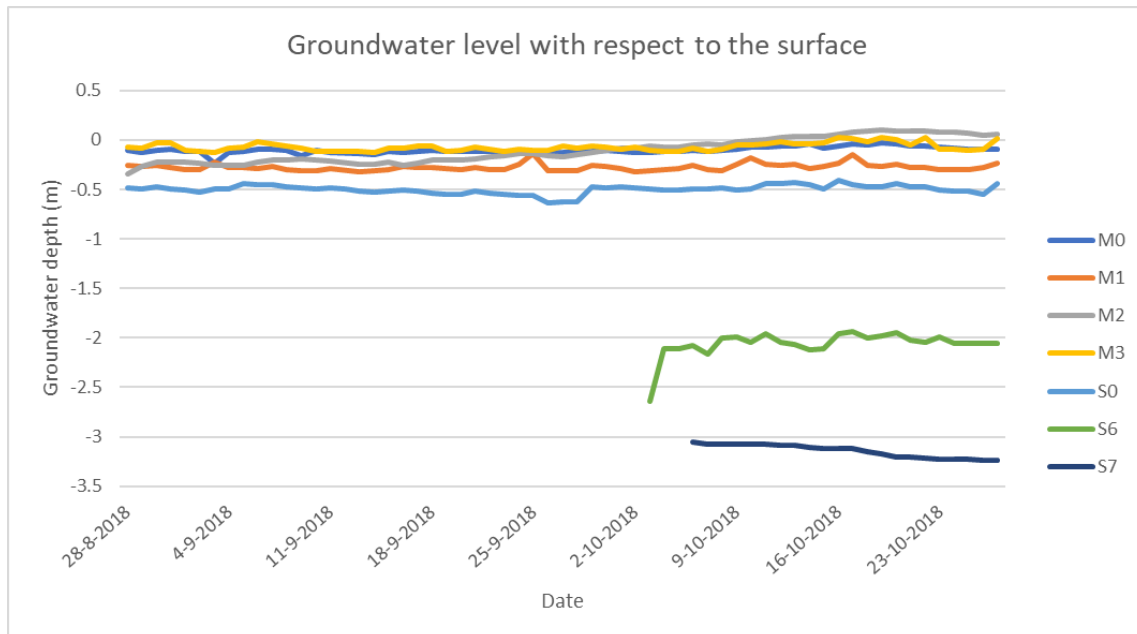


Figure 5.1: Groundwater levels in piezometers with respect to the ground surface (=0)

Almost all piezometers installed on the stable slopes were dry because they were not deep enough. S6 and S7 were installed on stable slope S1 at a later date and were deeper than S5 and S4 nearby. Figure 5.1 shows the groundwater table of the stable slope is fairly deep, and the depth increases from S0 upslope, to S7 near the river. S0, which was installed just upslope of the well, was the only piezometer on the stable slopes with a fairly high groundwater table. The groundwater table on the moved slope is just beneath the surface, and towards the end of the time series the water level in piezometer M2 is even slightly higher than the ground surface, indicating ponding. This is reasonable since the surface of the moved slope is much closer to the groundwater table and infiltration is high as well because of the disturbed soil. A schematic of the groundwater level in piezometers on the moved slope and stable slope S1 can be found in Appendix B.

From this schematic it becomes clear that the depth of the groundwater table increases from the well (stable slope) or the scarp (moved slope) to the river. The river has excavated its way through the landscape which makes that there is a significant (3-5m) drop from the toe of the slopes to the riverbed. This low-lying river could have a significant influence on the groundwater level of the surrounding slopes.

When comparing figure 5.1 to the rainfall data (fig. 5.2) no direct correlation is visible. Due to some initial errors in the rain gauge set up, the data from figure 5.2 comes from a rain gauge already set up at the nearby Nyabihu tea factory, less than 1km away. Though the groundwater table in the piezometers fluctuates from day to day there seems to be no evident relation to the fluctuations in rainfall. The relation between precipitation and groundwater recharge, however, is rarely straightforward since there are many more processes involved. To be able to correlate the rainfall data to the groundwater table more insight is needed in the specific processes taken place on these slopes, and probably a more extensive measuring period is required including at least one complete rainy season.



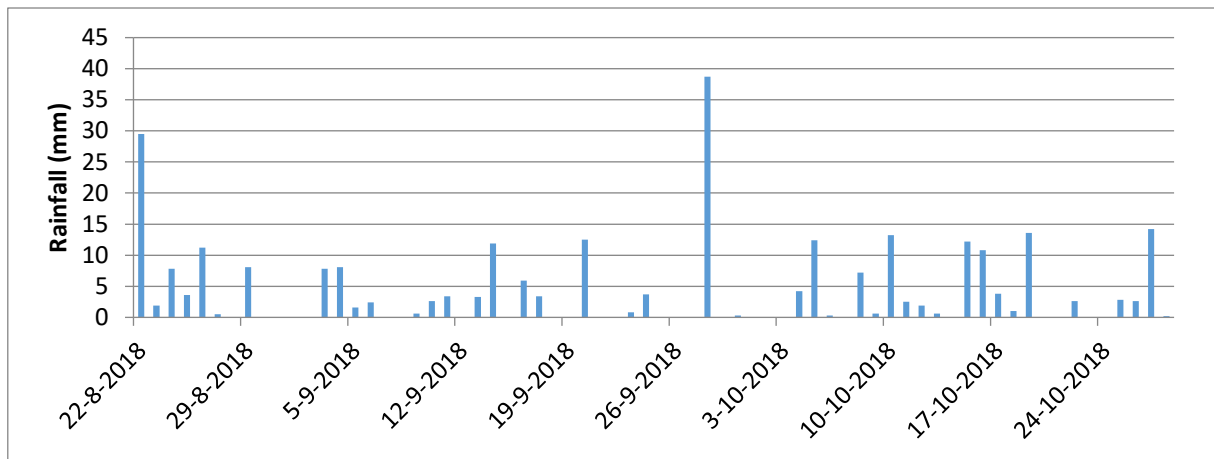


Figure 5.2: Precipitation data from August 22<sup>nd</sup> 2018 to October 29<sup>th</sup> 2018

## 5.2 Soil moisture tubes

Tables 5.1-5.5 summarize soil moisture measurements at the different locations from August 28<sup>th</sup> until October 28<sup>th</sup>. All the soil moisture tubes show considerable differences in average volumetric water content between the different measurement depths. Though differences in water content can be expected, especially between different soil layers, most of the measurement points lie in the top layer which make the differences between measurement depths odd. Correct installation is vital to produce optimal contact between the soil wall and the access tube. The augered holes should be straight and smooth and have the correct diameter. The large differences in readings can hence be due to improper installation leading to e.g. air pockets retained around the tube shaft. Such considerable differences in volumetric water content within one soil layer make it difficult to say something about the soil's ability to retain water. In addition, the differences in volumetric water content between consecutive measurement times seem insignificant. The Delta-T PR2 probe has an accuracy of 3% VWC. Often the difference between consecutive days is much smaller than that. For some measurement depths the largest difference for the whole time series isn't even larger than 3% showing practically no reaction to precipitation events, with the exception of 1-4 anomalies (of  $\pm 60$  measurement times) which were left out in the tables below.

T0 (open field; near well)				
Depth w.r.t. ground surface (m)	Average Volumetric Water Content (%)	Largest difference in VMC for total time series (%)	Largest difference in VMC between 2 consecutive days (%)	Standard deviation
-0.06	UnderRange	UnderRange	UnderRange	UnderRange
0.04	33.5	7.9	3.0	1.93
0.14	31.8	11.6	6.1	2.60
0.24	47.6	8.5	5.2	1.49
0.44	16.6	2.1	1.0	0.48
0.84	41.6	3.4	2.1	0.66

T1 (full grown; near S4)				
Depth w.r.t. ground surface (m)	Average Volumetric Water Content (%)	Largest difference in VMC for total time series (%)	Largest difference in VMC between 2 consecutive days (%)	Standard deviation
-0.105	UnderRange	UnderRange	UnderRange	UnderRange
-0.005	6.0	10.0	7.2	2.71
0.095	8.9	3.2	1.4	0.54
0.195	UnderRange	UnderRange	UnderRange	UnderRange
0.395	UnderRange	UnderRange	UnderRange	UnderRange
0.795	28.9	7.0	2.7	1.18

T2 (coppices; near S5)				
Depth w.r.t. ground surface (m)	Average Volumetric Water Content (%)	Largest difference in VMC for total time series (%)	Largest difference in VMC between 2 consecutive days (%)	Standard deviation
-0.005	UnderRange	UnderRange	UnderRange	UnderRange
0.095	27.1	4.4	2.7	1.05
0.195	15.5	3.5	2.0	0.58
0.295	28.8	8.1	3.9	1.37
0.495	46.5	7.7	6.2	1.35
0.895	31.0	5.1	2.5	0.68

T3 (coppices; near S2)				
Depth w.r.t. ground surface (m)	Average Volumetric Water Content (%)	Largest difference in VMC for total time series (%)	Largest difference in VMC between 2 consecutive days (%)	Standard deviation
-0.115	UnderRange	UnderRange	UnderRange	UnderRange
-0.015	UnderRange	UnderRange	UnderRange	UnderRange
0.085	27.0	7.9	3.0	2.01
0.185	2.2	2.1	0.8	0.51
0.385	24.8	2.0	1.5	0.58
0.785	17.8	4.8	2.5	0.87

T4 (full grown; near moved slope)				
Depth w.r.t. ground surface (m)	Average Volumetric Water Content (%)	Largest difference in VMC for total time series (%)	Largest difference in VMC between 2 consecutive days (%)	Standard deviation
-0.110	UnderRange	UnderRange	UnderRange	UnderRange
-0.010	0.9	3.0	-	0.87
0.090	35.2	9.2	3.4	2.25
0.190	14.9	4.8	2.0	1.20
0.390	23.7	4.9	2.3	1.22
0.790	33.2	8.2	3.5	1.92

Tables 5.1-5.5: Averages of soil moisture readings at different depths for tubes at different locations, including processed data.

### 5.3 Soil characteristics

The information gathered from the two pits that were dug on the stable slopes, and from the scarp of the moved slope are summarized in figures 5.3-5.5. The figures show a description of each soil layer with their respective depths.

#### Hydraulic conductivity

The values for the saturated hydraulic conductivity of each layer are also given. Not all layers were tested using both the laboratory constant head test and the in-situ inverse auger hole test. Some very gravelly layers in the stable slope were unsuited for the inverse auger hole test, as was the scarp of the moved slope. The constant head test is omitted for some layers because it was impossible to retrieve an undisturbed sample. The calculations made to convert the raw data assembled to a K-value can be found in Appendix C. In most cases the saturated hydraulic conductivity found through the inverse auger hole test is much lower than for the constant head test. The values for the inverse auger hole test are also more realistic. This is due to the fact that in the field the scale at which the test takes place (i.e. the surface area of soil in contact with the water column) is a lot larger and more representative than a small core sample ring in the laboratory. In addition, even though the soil surrounding the auger hole may be slightly smeared, it is often still much less disturbed than when a sample ring with soil is transported from the field to the laboratory. The  $K_{sat}$  values of the inverse auger hole test are also in coherence with the description made by touch and sight in the field. The  $K_{sat}$  values measured by the inverse auger hole test are high for the more 'sandy' layers, and more 'clayey' layers yield lower results. According to De Smedt (2013), based on hydraulic conductivity measured through the constant head test, most soil layers can be classified as medium sand ( $K = 8.64 \text{ m/d} - 0.864 \text{ m/d}$ ), and based on the inverse auger hole test most soil layers classify as fine sand ( $K = 0.864 \text{ m/d} - 0.0864 \text{ m/d}$ ). The

exception is slope S1 layer 3, which according to De Smedt (2013) classifies as coarse silt ( $K = 0.0864 \text{ m/d} - 0.00864 \text{ m/d}$ ).

#### *Infiltration*

Double ring infiltrometer test were carried out in full grown eucalyptus forest, eucalyptus coppices, and agricultural field. Using Philip's (1957) equation from Cammeraat et al. (2001) yielded unrealistically high  $K_{\text{sat}}$  values ( $\pm 150 \text{ m/d}$ ). This is due to the fact that the Philip's equation becomes a bad estimator for the hydraulic conductivity if the diffusivity parameter,  $S$ , is really high. In this case it was between 45-90 indicating an extremely dry soil. Calculations of the infiltration rate can be found in Appendix C. The hydraulic conductivity can also be estimated by the field capacity during infiltration. Simply taking the infiltration rate that had been constant for a while near the end of the infiltrometer test yielded a bit better results, between  $2.88 \text{ m/d}$  and  $5.76 \text{ m/d}$ . These results are similar to the ones found with the inverse auger hole and constant head test.

#### *Soil moisture and dry bulk density*

The figures 5.3-5.5 also show the moisture content of each layer which was also determined in two ways, first an in-situ measurement using the Delta-T ML3 sensor, and secondly through the conventional method of oven drying the soil. Some differences may be due to the fact that the in-situ measurements were not taken the same day as the samples for oven drying were collected. Looking at the results from oven drying the soil moisture content of the stable slopes are irregular, whereas for the moved slope the soil moisture content increases with depth of soil layer.

The dry bulk density is also determined (figs. 5.3-5.5) with the exception of some bottom layers for which no undisturbed sample could be taken for analysis. Most of the S0 and S1 soil layers have dry bulk densities average for sand. The top layer classifies more as an organic soil type. The layers of the moved slope can classify as sand or as a medium hard clay (De Smedt, 2013). Moreover, for the stable slopes the bulk density increased with soil layer depth, whereas for the moved slope it decreased. Though it may be unjust to draw direct conclusions from these data it must be noted that the moved slope is 'top heavy' and has a high soil moisture content in the lower layers which would signify a higher pore water pressure, and thus a lower effective shear strength.

Finally, the results of the direct shear test can also be found in figures 5.3-5.5. A discussion of these results can be found in the next chapter, Back analysis of slope stability. An example of the direct shear results for the moved slope M can be found in Appendix I.

0	<b>Black humic layer  Roots present   Loose</b>			Infiltration capacity: 2.88 m/d
	<u>Hydraulic conductivity</u>	<u>Soil moisture content</u>	$C = 7.46 \text{ kPa}$	Dry bulk density: 819 kg/m <sup>3</sup>
	5.83 m/d (constant head)	28.3% (in situ)	$\phi = 40.8^\circ$	
0.15	1.71 m/d (inv. auger hole)	15% (after drying)		
	<b>Brown-yellow mixture of sand and silt   Roots present   Hard</b>			Dry bulk density: 1686 kg/m <sup>3</sup>
	<u>Hydraulic conductivity</u>	<u>Soil moisture content</u>	$C = 39.11 \text{ kPa}$	
	2.50 m/d (constant head)	11% (in situ)	$\phi = 30.2^\circ$	
0.65	0.16 m/d (inv. auger hole)	9% (after drying)		
	<b>Whitish quartz material  No roots   Dry   Compact</b>			Dry bulk density: 1695 kg/m <sup>3</sup>
	<u>Hydraulic conductivity</u>	<u>Soil moisture content</u>	$C = 87.69 \text{ kPa}$	
	1.11 m/d (constant head)	9.5% (in situ)	$\phi = 8.1^\circ$	
1.75	- m/d (inv. auger hole)	17% (after drying)		
	<b>Blackish soil   Some roots   mixture of layer 1 &amp; 3   Hard   Wet</b>			Dry bulk density: 1635 kg/m <sup>3</sup>
	<u>Hydraulic conductivity</u>	<u>Soil moisture content</u>	$C = 29.71 \text{ kPa}$	
	2.22 m/d (constant head)	12.2% (in situ)	$\phi = 14.3^\circ$	
1.95	0.5 m/d (inv. auger hole)	8% (after drying)		
	<b>Whitish quartz material  No roots   Dry   Compact</b>			
	<u>Hydraulic conductivity</u>	<u>Soil moisture content</u>	$C = 26.04 \text{ kPa}$	
	- m/d (constant head)	3.1% (in situ)	$\phi = 34.6^\circ$	
	0.5 m/d (inv. auger hole)	- % (after drying)		

Figure 5.3: Description of soil layers of pit S0, including hydraulic conductivity, soil moisture content, bulk density, and direct shear results

0	<b>Dark brown silty soil   Roots present   Loose</b>			Infiltration capacity: 5.76 m/d
	<u>Hydraulic conductivity</u>	<u>Soil moisture content</u>	$C = 10.54 \text{ kPa}$	Dry bulk density: 1080 kg/m <sup>3</sup>
	0.28 m/d (constant head)	31.6% (in situ)	$\phi = 24.7^\circ$	
0.95	0.4 m/d (inv. auger hole)	13% (after drying)		
	<b>Orange, coarse gravel with clay   No roots   Very hard   Large stones present</b>			Dry bulk density: 1693 kg/m <sup>3</sup>
	<u>Hydraulic conductivity</u>	<u>Soil moisture content</u>	$C = 18.42 \text{ kPa}$	
	2.78 m/d (constant head)	8% (in situ)	$\phi = 37.9^\circ$	
1.65	- m/d (inv. auger hole)	9% (after drying)		
	<b>Lighter colored, smaller gravel with more sand and clay  No roots   Hard</b>			Dry bulk density: 1726 kg/m <sup>3</sup>
	<u>Hydraulic conductivity</u>	<u>Soil moisture content</u>	$C = 39.61 \text{ kPa}$	
	0.37 m/d (constant head)	15.9% (in situ)	$\phi = 44.1^\circ$	
2.40	0.03 m/d (inv. auger hole)	10% (after drying)		
	<b>Yellow sand   No roots   Compact</b>			
	<u>Hydraulic conductivity</u>	<u>Soil moisture content</u>	$C = 19.49 \text{ kPa}$	
	- m/d (constant head)	17.2% (in situ)	$\phi = 33.9^\circ$	
3.25	0.6 m/d (inv. auger hole)	- % (after drying)		

Figure 5.4: Description of soil layers of pit S1, including hydraulic conductivity, soil moisture content, bulk density, and direct shear results

0	<b>Light colored   Clayey soil deposited for construction   No roots   Compact</b>			Dry bulk density: 1959 kg/m <sup>3</sup>
	<u>Hydraulic conductivity</u>	<u>Soil moisture content</u>	$C = 18.53 \text{ kPa}$	
	2.58 m/d (constant head)	20.6% (in situ)	$\phi = 27.6^\circ$	
4.80	- m/d (inv. auger hole)	13% (after drying)		
	<b>Light colored clay   No roots   Very hard</b>			Dry bulk density: 1762 kg/m <sup>3</sup>
	<u>Hydraulic conductivity</u>	<u>Soil moisture content</u>	$C = - \text{kPa}$	
	2.78 m/d (constant head)	18.6% (in situ)	$\phi = -^\circ$	
5.50	- m/d (inv. auger hole)	17% (after drying)		
	<b>Yellowish sand   No roots   Very hard</b>			Dry bulk density: 1658 kg/m <sup>3</sup>
	<u>Hydraulic conductivity</u>	<u>Soil moisture content</u>	$C = - \text{kPa}$	
	1.87 m/d (constant head)	16.4% (in situ)	$\phi = -^\circ$	
6.10	- m/d (inv. auger hole)	21% (after drying)		
	<b>Light colored clay   No roots   Hard</b>			Dry bulk density: 1672 kg/m <sup>3</sup>
	<u>Hydraulic conductivity</u>	<u>Soil moisture content</u>	$C = 0 \text{ kPa}$	
	2.22 m/d (constant head)	21.3% (in situ)	$\phi = 49.7^\circ$	
6.90	- m/d (inv. auger hole)	24% (after drying)		
	<b>Light colored clay   No roots   Softish   Wet</b>			Dry bulk density: 1615 kg/m <sup>3</sup>
	<u>Hydraulic conductivity</u>	<u>Soil moisture content</u>	$C = 11.38 \text{ kPa}$	
	1.32 m/d (constant head)	33% (in situ)	$\phi = 40.4^\circ$	
	- m/d (inv. auger hole)	26 % (after drying)		

Figure 5.5: Description of soil layers of the scarp of the moved slope, including hydraulic conductivity, soil moisture content, bulk density, and direct shear results

## 5.4 Soil texture

Figure 5.6 shows the grainsize distributions of the slip surface soil layer of landslides nr. 50, 128, 187, and 219. Figures 5.7-5.9 show the grainsize distribution for all the layers of the moved slope and the two stable slopes of the Karago landslide, nr. 63.

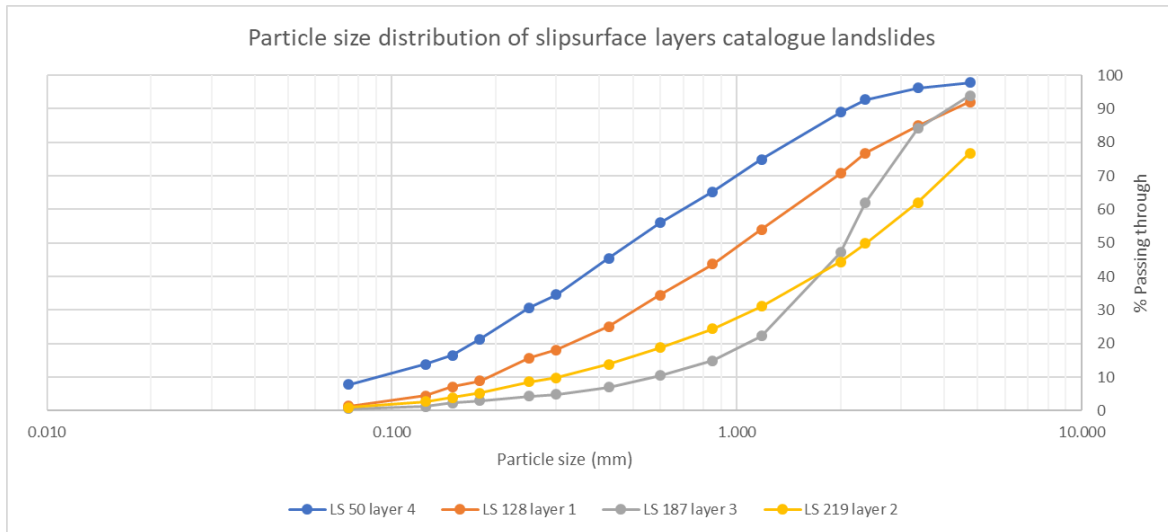
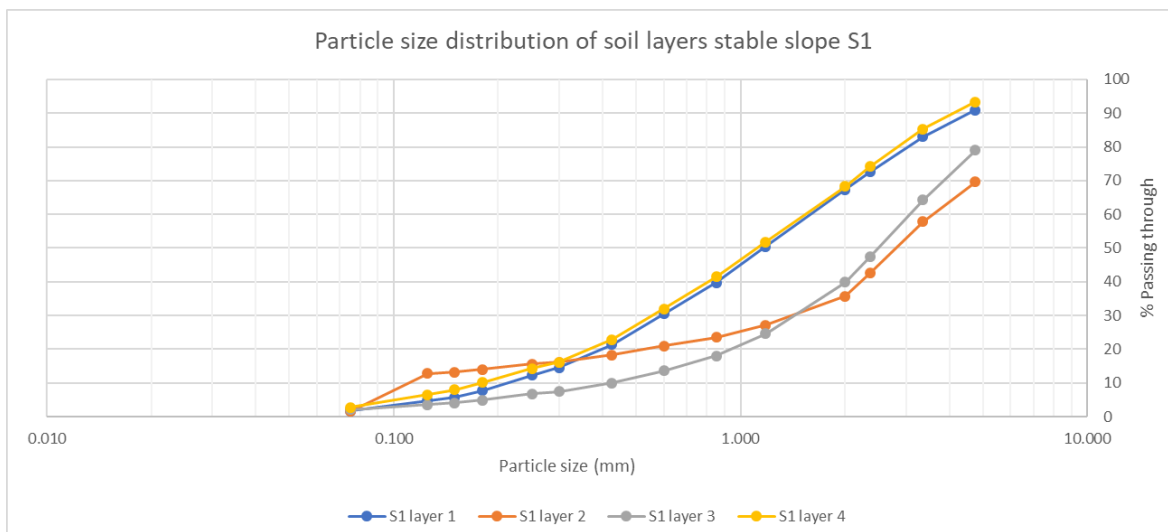
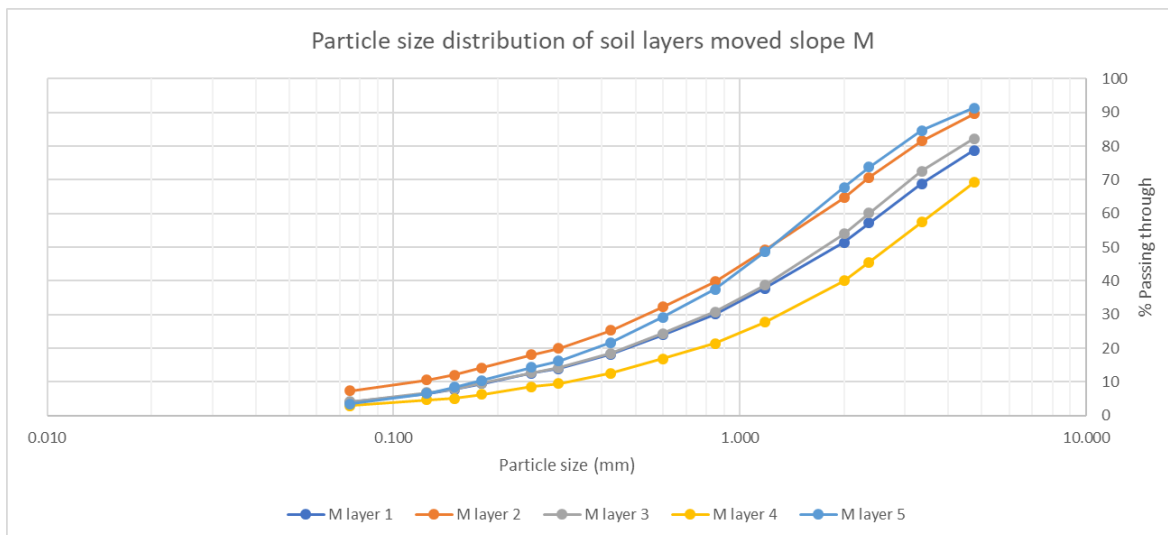


Figure 5.6: Particle size distribution of slip surface layers of regional landslides



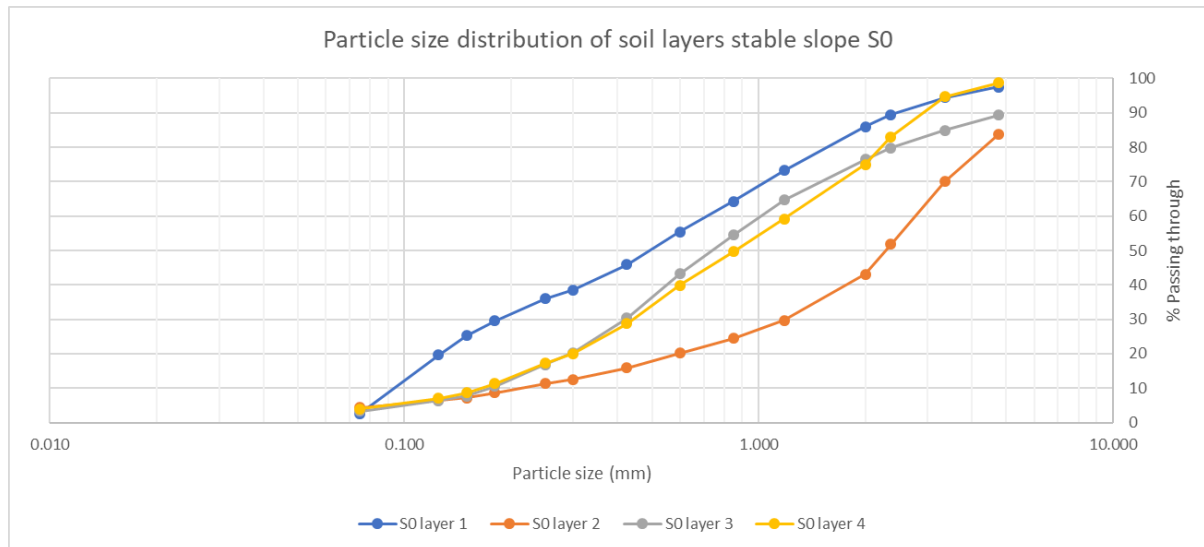


Figure 5.7-5.9: Particle size distribution of soil layers of moved slope M, stable slope S0 and stable slope S1

To classify the soils the criteria of the Unified Soil Classification System was applied. An overview of the procedure can be found in Appendix D. Some criteria are summarized here.

- Texture: *coarse grained* soil if >50% is retained by nr. 200 sieve (0.075mm)
- Main property: *sand* if <50% of coarse fraction is retained by nr. 4 sieve (4.75mm). Otherwise, *gravel*
- Fines fraction: in case of sand, if fines fraction <5% soil is well graded or poorly graded. If fines >12% soil is silty or clayey
- Particle distribution: in case of sand, if  $C_u > 6$  and  $1 < C_c < 3$  sand is well graded. Otherwise, poorly graded.

$$C_u = \frac{D_{60}}{D_{10}} \quad (5.1)$$

$$C_c = \frac{(D_{30})^2}{D_{10}D_{60}} \quad (5.2)$$

Location	Layer	Texture (% retained by 0.075 mm)	Main property (% retained by 4.75 mm)	Fines fraction (% passing 0.075 mm)	Cu	Cc	D60 (mm)	D30 (mm)	D10 (mm)	Soil Description
LS50	L4	92.23	2.20	7.77	7.59	0.91	0.708	0.245	0.093	SP-SM
LS128	L1	98.61	7.97	1.39	7.65	0.94	1.472	0.517	0.192	SP
LS187	L3	99.47	6.02	0.53	4.01	1.55	2.310	1.435	0.576	SP
LS219	L2	99.11	23.22	0.89	10.43	1.31	3.183	1.129	0.305	SW
M	L1	95.97	21.26	4.03	13.60	1.43	2.603	0.845	0.191	SW
	L2	92.68	10.36	7.32	15.09	1.46	1.753	0.544	0.116	SP-SM
	L3	95.91	17.75	4.09	12.36	1.51	2.350	0.822	0.190	SW
	L4	97.10	30.77	2.90	11.44	1.53	3.648	1.335	0.319	SW
	L5	96.59	8.62	3.41	9.58	1.34	1.666	0.623	0.174	SW
S0	L1	97.37	2.48	2.63	7.55	0.48	0.729	0.184	0.097	SP
	L2	95.69	16.36	4.31	12.98	2.38	2.804	1.200	0.216	SW
	L3	96.69	10.69	3.31	5.89	0.98	1.029	0.420	0.175	SP
	L4	96.07	1.26	3.93	7.40	0.98	1.222	0.444	0.165	SP
S1	L1	98.29	9.11	1.71	7.64	0.99	1.642	0.591	0.215	SP
	L2	98.46	30.42	1.54	32.00	5.17	3.609	1.450	0.113	SP
	L3	97.96	20.98	2.04	7.27	1.64	3.099	1.471	0.426	SW
	L4	97.21	6.60	2.79	8.86	1.12	1.585	0.563	0.179	SW

Table 5.6: Soil texture analysis results

The resulting soil descriptions in table 5.6 show that based on the USCS all the soil layers investigated can be classified as sand, either well graded or poorly graded. Two layers classify as silty sand. This analysis seems to differ substantially on some points with description based on observation in figures 5.3-5.5, especially for the moved slope. To classify all the soils as a sand also has consequences for the analysis of the direct shear results discussed in the next chapter.

Although the fines fraction in almost all soil layers is too small to classify as anything below sand, there are fines present. Appendix E shows the results of the Atterberg limits tests for the soil layers of the Karago landslide. Though the soil layers overall have low plasticity, indicating the relative response of the soil layer to deformation, and the plasticity tends to decrease further with soil layer depth, fines are present and do have a contribution to soil properties such as cohesion, and hydraulic conductivity as seen before.



## 6. Back analysis of slope stability

In this chapter the data from the direct shear test and particle size analysis is further analysed using the spreadsheet SLIP5EX. The aim is to be able to answer the second research question; find out the response of the hillslopes using the hydrological and geotechnical data collected.

SLIP5EX calculates the factor of safety using the infinity slope method, and Fellenius' method. The input arguments for this are the geometry (length, angle, depth of slip surface, water table, and depth of different layers), the soil density properties, and the cohesion and angle of internal friction. Since SLIP5EX can only register three soil layers, the bottom most layer from a landslide (often containing the slip surface) corresponds to layer 3 in SLIP5EX, the second most bottom layer corresponds to layer 2, and the third most bottom layer to layer 1 in the spreadsheet. This is done because the cohesion and angle of internal friction of deeper layers have a larger effect on slope movement. Only Fellenius' method takes into account the properties of soil layers above the slip surface, the infinite slope method does not. A screenshot of the spreadsheet can be found in Appendix F.

For the landslides of the regional assessment the moist and saturated bulk unit weight were only determined for the soil layer that holds the slip surface. For layers above the slip surface the unit weights and the cohesion and angle of internal friction were estimated by comparing the soil type to that of a layer of the Karago landslide since there data was gathered for all soil layers.

Table 6.1 summarizes the results of all 3 runs of SLIP5EX made for each hillslope. The only difference between the runs is the value of the cohesion and angle of internal friction. The first run is made using the cohesion and angle of internal friction as found through the direct shear test. Often these yielded factors of safety much higher than 1. In the second run the cohesion and angle of internal friction were changed manually so that the factor of safety was exactly 1 (or as close as possible). The values used were kept as realistic as possible. The third run used typical values for the soil type as cited by literature (De Smedt, 2013). The soil type was primarily determined by the density measurements and the particle size analysis. If for a certain soil type a range of typical values were given by the literature used, the value used was chosen such that the factor of safety came as close to 1 as possible.

Slope / landslide		C layer1 (kPa)	$\phi$ layer1 (°)	C layer2 (kPa)	$\phi$ layer2 (°)	C layer3 (kPa)	$\phi$ layer3 (°)	F (Fellenius)	F (ISM)
LS50	Direct shear results	39.1	30.2	39.6	44.1	36.4	30.6	2.99	1.92
	Manual iteration	0	15	0	20.5	0	25	1	1
	Literature value	0	<30	0	30-32.5	0	<30	1.12	1
LS128	Direct shear results	9.2	33.7	9.2	33.7	19.5	33.9	1.23	0.97
	Manual iteration	1	31	1	31	0	38	1	1
	Literature value	0	<30	0	<30	0	32.5-35	0.92	0.9
LS187	Direct shear results	39.1	30.2	39.6	44.1	0	41	3.75	1.04
	Manual iteration	0	0	0	0	2	38	1.78	0.99
	Literature value	0	<30	0	35-37.5	0	32.5-35	1.88	0.83
LS219	Direct shear results	10.5	24.7	27.7	31.6	50.2	41.1	2.46	1.6
	Manual iteration	0	0	2	38	0	37	1.25	0.99
	Literature value	0	<30	0	35-37.5	0	35-37.5	1.03	0.83
M	Direct shear results	41.73	29.8	0	49.7	11.4	40.4	1.9	1.44
	Manual iteration	0	26	0	33	2	33	1	1
	Literature value	0	32.5-35	0	32.5-35	0	30-32.5	1.05	0.96
S0	Direct shear results	87.7	8.1	29.7	14.3	26	34.5	3.74	1.92
	Manual iteration	0	30	0	35	2	34.5	1	1
	Literature value	0	30-32.5	0	35-37.5	0	30-32.5	0.90	0.86
S1	Direct shear results	18.4	37.9	39.6	44.1	19.5	33.9	2.28	1.63
	Manual iteration	0	27	0	30	0	34.5	1	1
	Literature value	0	30-32.5	0	32.5-35	0	35-37.5	1.04	1.02

Table 6.1: Results of 3 runs of the spreadsheet SLIP5EX (using direct shear results, manual iteration to come to a factor of safety of 1, and using values from literature) for all landslides analysed.

*LS50* - using the direct shear results yielded factors of safety of 2.99 (Fellenius) and 1.92 (ISM). For the manual iteration low angles of internal friction were required to achieve a factor of safety of 1. The soil layer in which the slip surface was located classified as SP – SM, between poorly graded sand and silty sand, so they may have well been cohesion between the grains. This could have led to a higher factor of safety when using the corresponding values from literature. This could be an indication that the slope may not have failed entirely due to internal factors but possibly because of external factors such as excavation for brick making.

*LS128* – using both the direct shear results and the values from literature yield factors of safety below 1, with the exception of Fellenius' method when using direct shear results. The difference in factor of safety comes primarily from the difference in calculation method since the slip surface is taken to be at the contact point between layers 2 (same as layer 1) and 3.

*LS187* – using the direct shear results yielded factors of safety of 3.75 (Fellenius) and 1.04 (ISM). The cohesion of layer 3 is set to 0 because the y-intercept of the trendline of the Mohr-Coulomb envelope was negative. For this particular landslide the difference between Fellenius' method and the ISM is particularly large. As can be seen in table 6.1., even when C and  $\phi$  values of the layers above are both manually set to unrealistic values of 0, the factor of safety according to Fellenius is still 1.78. This is due to the fact that the ISM is particularly useful for the assessment of shallow landslides, where the length to depth ratio of a landslide is larger than 10, or even 25 (Bogaard & Greco, 2015). For LS187 the length to depth ratio is only 1.75

*LS219* - using the direct shear results yielded factors of safety of 2.46 (Fellenius) and 1.60 (ISM). Once again the values of C and  $\phi$  for the layer containing the slip surface (layer 2) were too high. The C and  $\phi$  values for layers 1 and 3 were based on direct shear tests of similar soil type from the Karago landslide. Manually setting both C and  $\phi$  of layer 1 to unrealistic values of 0 once again doesn't achieve a factor of safety of 1 using Fellenius' method. The properties of layer 3 are actually irrelevant since it is beneath the slip surface. Table 6.1 shows that with realistic values for the soil type, based on the soil texture analysis, a factor of safety close to, or smaller than 1 can be achieved indicating slope failure can be due to internal properties.

*Moved slope* – using the C and  $\phi$  values from the direct shear test the factors of safety using Fellenius and the infinite slope method (ISM) are 1.9 and 1.44 respectively. The cohesion of layer 2 is set to 0 because the y-intercept of the trendline of the Mohr-Coulomb envelope was actually negative. For the manual iteration the cohesion for layer 1 and 2 was set to 0 because these were classified as sand. Although layer 3 also was classified as sand based on texture analysis, in the field it felt a lot like clay, and therefore it was given a slight cohesive property of 2 kPa.

*Stable slope S0* – using the direct shear results the obtained factors of safety are 3.74 (Fellenius) and 1.92 (ISM). It can be said that the slope is rightly stable. Nonetheless, some values from the direct shear test are unrealistically high (C layer1 = 87.7 kPa). In this case the reason could be that this layer contained very much gravel thereby giving distorted test results. When using the values from literature, which were primarily based on the saturated bulk unit weight of the layers, the slope actually has factors of safety smaller than 1. However, just as was the case for the moved slope, the gravelly layers felt quite sticky due to clay like material in between, which would give the soil a cohesion higher than 0. Another could be that the depth of the slip had to be estimated for this stable slope and was now taken as the plane between the bedrock and the top soil.

*Stable slope S1* - using the direct shear results the obtained factors of safety are 2.28 (Fellenius) and 1.63 (ISM). It can be said that the slope is rightly stable, though once again the direct shear results were quite high. In this case however, the values from literature yield a factor of safety only just above 1.

## 7. Discussion

### *Direct shear*

Of the slopes analysed only S0 and S1 didn't move, which mean they rightly should have a safety factor higher than 1. For the other slopes the safety factor should be very close to, or below, 1. Almost all the runs with the direct shear results yield safety factors much higher than 1, which means the direct shear test and results should be analysed more closely. Direct shear tests have some limitations in the case of coarse-grained material. Particles sizes must be small enough to avoid boundary effects in a small shear box. However, if the particles become too large (approx.  $> 1/10$  shear box diameter) the test will actually yield the  $C$  and  $\phi$  values of individual grains and not a soil skeleton. The shear strength of particles rolling and sliding over each other is often much lower than that of an individual grain. Some soil layers contained very much gravel which was not always visible when inserting the sample in the shear box, but could well be noticed as sometimes the shear strength would build up without a horizontal displacement taking place indicating the shearing of a piece of gravel. Suddenly the shear strength would drop which meant the gravel particle had failed. In this way the  $C$  and  $\phi$  are greatly over estimated for coarser grained soils.

The strength of the soil is also heavily dependent on the level of saturation and consolidation. Most samples were taken undisturbed from a sampling box and only reconsolidated a little bit before testing. Other samples that were disturbed were often consolidated by more than the normal force applied during testing, but only for a short period prior to testing. It may be that these samples expanded easily during testing, thereby decreasing the soil strength. The vertical displacement of the sample during testing gives an indication of how densely packed the soil is. For some layers there was a clear difference in vertical displacement pattern for tests at different normal loadings. How densely a soil is packed also has an influence on the direct shear strength and over consolidation could hence lead to overestimated cohesion values.

Complete saturation is also essential for the consolidated drained tests. If the sample is not completely saturated the effective stress could be falsely lower. Since only three points are used to plot a best fit line for the Mohr-Coulomb failure envelope, a discrepancy in one of the points can already change the cohesion and angle of internal friction a lot.

### *Literature values and soil classification*

When doing the manual iteration to obtain a safety factor of 1, the values for  $C$  and  $\phi$  used are often close to literature values used from De Smedt (2013) (See Appendix G). The choice for these literature values is based on the grainsize analysis, and furthermore the bulk density test. Using these values for  $C$  and  $\phi$  yields a safety factor of (close to) 1. Thus, very low (or 0)  $C$  values and relatively high  $\phi$  values, as used in the manual iteration, are consistent with what has been reported in literature, and, with the applied geometry, could rightly reflect slope failure ( $F \leq 1$ ).

Nevertheless, the values from literature offer a range, and are therefore quite crude. Based on field observations and the (although small) fraction of fines retained by 0.075mm sieve in the texture analysis it would be realistic to at least expect some cohesion for certain layers. As reported above there are several explanations as to why the direct shear tests yield such high values, but these are probably not enough to eradicate the presence of cohesion completely in all layers. The cohesion may be small, but to assume no cohesion at all would not be in line with field observations, the presence of fines, and some  $K_{sat}$  results. Even though the fines fraction may be small, it can still have a significant influence on the slope stability. Conversely, the fact that at the slip surface such a low cohesion is required to make a slope fail does not mean the entire soil layer or slope has low, or no, cohesion. The slope will most likely fail at its weakest point. This could be a very thin layer, an anomaly, or a result of heterogeneity, such as large pores, in the soil. To retrieve such a small weak layer is, however, nearly impossible, especially after the slope has failed.

Another explanation for the large discrepancy between direct shear results and literature values can lie in the cause of failure. So far, the assumption has been that the slope has to fail due to internal causes, such as a low  $C$  and  $\phi$ . Thus, when using the direct shear results would never fail, based on the

safety factor. However, as can be seen in Appendix H, the possible cause of failure is not always internal. Based on observation and conversations with locals the cause may have been excavation for road fixing (LS187) or brick building (LS50), or perhaps the fact that there was a big drain through the field caused the washing out of the toe (LS219).

#### *SLIP5EX sensitivity analysis*

For each slope the only variables that were changed between different runs were the cohesion and angle of internal friction. The geometry was not changed, and although input parameters such as the contact points between layers are fairly easy to measure in the field, the slope angle and depth of slip plane were quite difficult to measure (or estimate) accurately. In SLIP5EX this ambiguity around certain parameters translates into a sensitivity, for which a sensitivity analysis can be portrayed in a figure, such as figure 7.1. Based on the coefficient of variability assigned to each parameter, the effect of changing that parameter, on the factor of safety can be obtained.

The coefficients of variability predominantly used were: 20% for bulk unit weight, 10% for soil and groundwater depth, 30% for slope angle, 100% for cohesion, and 50% for angle of internal friction. For bulk unit weight and soil depth this was based on the variability in measurement results, and how easy it was to actually measure these parameters. The slope angle was taken from the landslide inventory and only gave a range (i.e. 32-45°). Since the slope angle was not measured exactly when revisiting the field, it was estimated, and therefore holds quite a high coefficient of variability. For the cohesion and angle of internal friction the coefficient of variability was based on the variability in direct shear results. Since these were extremely high for the cohesion and a little bit less high for the angle of internal friction 100% and 50% were used respectively.

For the particular case of LS50 (fig. 7.1) it can be seen that a small change in the slope angle (x-axis) already brings about a large change in the safety factor (y-axis). The exact value by which the factor of safety changes also depends on the value of the input parameter, and may thus be slightly different for other landslides. However, the slope of the lines in figure 7.1 remain roughly the same, and say the most about the influence of each parameter. Hence, by changing other parameters than C and  $\phi$  a significant change in safety factor can be achieved, allowing C and  $\phi$  to be set to more realistic values in some cases, to achieve a safety factor of 1.

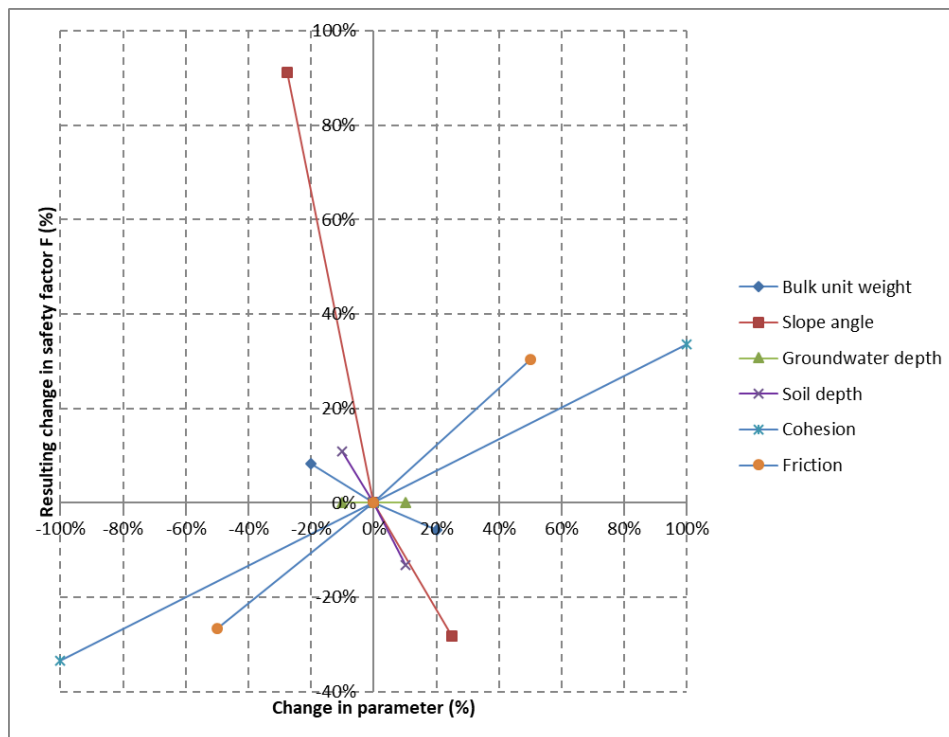


Figure 7.1: Sensitivity analysis of the SLIP5EX input parameters for landslide nr. 50

## 8. Conclusion

During the fieldwork part of this project abundant geotechnical data, such as soil texture, cohesion, and angle of internal friction, was mapped. A fair amount of hydrological data, such as the hydraulic conductivity, the infiltration capacity, the groundwater level, and the soil moisture content, was also gathered for one of the five landslides investigated. Although not all the data was in agreement, it gave good insight into the hydrogeotechnical characteristics of these landslides.

Based on the soil texture analysis all the landslides occurred in sandy, and occasionally slightly silty, soil. For the Karago landslide this is supported by the results from the hydraulic conductivity and infiltration capacity, which are also typical for sandy soils. The cohesion measured, though it was often unrealistically high, indicated a very clayey soil, and the angle of internal friction, also unrealistically high sometimes, indicated a very sandy soil. Hence the results of the direct shear test are perhaps unlikely, but so are the results of the back analysis which often require a  $C$  of 0 for a slope to fail. This was clearly not the case either since there was always some clay present (based on soil texture analysis and field observation). As stated before, stable slopes are the rule, and failed slopes the exception. It only takes thin weak layer and a short trigger to offset a landslide. This may not be caught in the test results.

Based on the soil strength parameters from the direct shear results it could also be concluded that the reason for failure is not internal geotechnics, but possible external, anthropogenic, factors. Especially in Rwanda anthropogenic activities, such as road cutting or agricultural practices, can play a major role in landslide triggering. Therefore, it is also important to analyse not only the (failed) slopes, but also their surroundings closely. For the Karago landslide for example, the groundwater table is clearly influenced by the river at the toe. Groundwater plays a large role in the pore water pressure, and thus slope stability, and toe erosion of the slope due to the river does so as well. Therefore, it is important to analyse the whole picture and not only base causes of failure on individual tests.

The focus of the tests became more on geotechnics, which was analysed for all five landslides, rather than hydrology, which was only analysed for one location. Slope failure often has to do with the hydrology, so to assess the hydrological response of a slope more hydrological data will be required for other slopes as well, in order to be able to establish some relation between the geotechnics, hydrology, and slope movement. It is thus recommended to add hydrological measurements to other slopes as well. To really assess the hydrological response of a hillslope would require a much longer measurement time too, and more insight into the relation between precipitation, groundwater, infiltration and hillslope movement as well.

For future investigation it would be interesting to use the landslide distribution data from Uwihirwe (2018) as a starting point for further research. Most landslides occur at a certain elevation, with a slope angle of 25-32°. They are shallow (<1m) and take place on agricultural soil with a high clay content (>35%). It is worth investigating whether this is coherent with more detailed hydrogeotechnical analysis to be able to say whether these are indeed significant factors in landslide occurrence. From the tests in this report it is not evident that the underlying pegmatite lithology had an influence on the response of hillslopes. It is simply one of the two most abundant lithological units in North Western Rwanda and therefore also contains most landslides on it.

## Bibliography

- Bogaard, T.A. (2001). *Analysis of hydrological processes in unstable clayey slopes* (Doctoral dissertation). Universiteit Utrecht, Utrecht, Netherlands.
- Bogaard, T.A., & Greco, R. (2015). Landslide hydrology: from hydrology to pore pressure. *WIREs Water*, 3(3), 439-459. Doi: 10.1002/wat2.1126
- Brabb, E.E. (1991). The world landslide problem. *Episodes*, 14(1), 52-61.
- Cammeraat, L.H., Van Beek, L.P.H. & Dorren, L.K.A. (2001). *Eco-Engineering and Conservation of Slopes for Long Term Protection from Erosion, Landslide, and Storm*. Amsterdam, Netherlands.
- Clay, D.C., & Lewis, L.A. (2003). Land use, soil loss and sustainable agriculture in Rwanda. *Human Ecology*, 18(2), 147-161. doi: 10.1007/BF00889179
- Climate Musanze. (2018). Retrieved from <https://en.climate-data.org/africa/rwanda/majyaruguru/musanze-3390/>
- De Smedt, F. (2013) *Geomechanics*. Brussel: Vrije Universiteit Brussel.
- Kessler, J. & Oosterbaan, R. (1974). Determining hydraulic conductivity of soils. In H.P. Ritzema (Ed.), *Drainage principles and applications*. (pp. 253-256). Wageningen: International Institute for Land Reclamation and Improvement.
- Knapen, A., Kitutu, M.G., Poesen, J., Breugelmans, W., Deckers, J., & Muwanga, A. (2006). Landslides in a densely populated county at the footslopes of Mount Elgon (Uganda): Characteristics and causal factors. *Geomorphology*, 73(1), 149-165. doi: 10.1016/j.geomorph.2005.07.004
- Malamud, B.D., Turcotte, L.D., Guzzetti, F., & Reichenbach, P. (2004) Landslide inventories and their statistical properties. *Earth Surface Processes and Landforms*, 29(6), 687-711. Doi: 10.1002/esp.1064
- ML3 ThetaProbe Soil Moisture Sensor. (2018). Retrieved from <https://www.deltat.co.uk/product/ml3/>
- Nsengiyumva, J.B. Ministry of Disasters Management and Refugee Affairs. (2012). *Identification of Disaster Higher Risk Zones on Floods and Landslides*. Kigali: Republic of Rwanda.
- Persichillo, P., Bordoni, M., Meisina, C., Bartelletti, C., Giannecchini, R., D'Amato Avanzi, G., Galanti, Y., Cevasco, A., Brandolini, P., Galve, J.P., & Barsanti, M. (2016). Shallow landslide susceptibility analysis in relation to land use scenarios. In S. Aversa, L. Cascini, L. Picarelli & C. Scavia (Eds), *Landslides and Engineered Slopes. Experience, Theory and Practice*. (pp. 1605-1612). doi: 10.1201/b21520-199
- Philip, J.R. (1957). The theory of infiltration: 4. Sorptivity and algebraic infiltration equations. *Soil Science*, 84(3), 257-267.
- PR2 Profile Probe – analogue version. (2018). Retrieved from <https://www.deltat.co.uk/product/pr2/>

Reichenbach, P., Cardinali, M., De Vita, P., & Guzzetti, F. (1998). Regional hydrological thresholds for landslides and floods in the Tiber River Basin (central Italy). *Environmental Geology*, 35(2), 146-158. doi: 10.1007/s002540050301

TD-Diver. (2017). Retrieved from <https://www.vanessen.com/products/water-level/td-diver#description>

Uwihirwe, J. (2018) [Landslide distribution: causes and triggers in North Western Rwanda]. Unpublished report.

Van der Esch, S. PBL Netherlands Environmental Assessment Agency. (2017). *Exploring future changes in land use and land condition and the impacts on food, water, climate change and biodiversity*. The Hague: PBL Publishers.

Varnes, D.J. (1978). Slope movement types and processes. In R.L. Schuster & R.J. Krizek (Eds), *Transportation Research Board Report 176. Landslides. Analysis and control*. (pp. 11-33). Retrieved from <http://onlinepubs.trb.org/Onlinepubs/sr/sr176/176-002.pdf>

Varnes, D.J. (1984). *Landslide hazard zonation: a review of principles and practice*. Retrieved from <http://unesdoc.unesco.org/images/0006/000630/063038EB.pdf>

Verdoodt, A., & Van Ranst, E. (2003). *A large-scale land suitability classification for Rwanda*. Gent: Laboratory of Soil Science, Ghent University.

Verruijt, A. (2007) *Soil Mechanics*. Delft: VSSD.



## Appendices

### Appendix A – Additional piezometer data from Karago landslide

The height differences between the piezometers was measured using a levelling instrument. Due to the many changes of station because of the steeply sloped terrain there is an error margin in the readings. The actual elevation was measured using a smartphone app and is therefore not very accurate.

Piezometer label	Piezometer (top) elevation (m amsl)	Pipe length (m)	Distance above ground (m)	Ground elevation (m amsl)	Depth of piezometer below ground level (m)	Depth of piezometer (m amsl)
M0	2435.83	1.84	0.72	2435.11	-1.12	2433.99
M1	2430.65	1.83	0.64	2430.01	-1.19	2428.82
M2	2435.38	2	0.74	2434.64	-1.26	2433.38
M3	2441.00	2.4	0.68	2440.32	-1.72	2438.60
S0	2446.38	1.93	0.67	2445.71	-1.26	2444.45
S1	2432.18	1.7	0.8	2431.38	-0.9	2430.48
S2	2438.97	2.59	0.49	2438.48	-2.1	2436.38
S3	2448.29	1.9	0.52	2447.77	-1.38	2446.39
S4	2431.27	2.99	0.85	2430.42	-2.14	2428.28
S5	2439.89	2.83	0.93	2438.96	-1.9	2437.06
S6	2440.48	3.26	0.52	2439.96	-2.74	2437.22
S7	2433.12	4.24	0.83	2432.29	-3.41	2428.88

## Appendix B – schematic of groundwater level in piezometers on slope M and S1

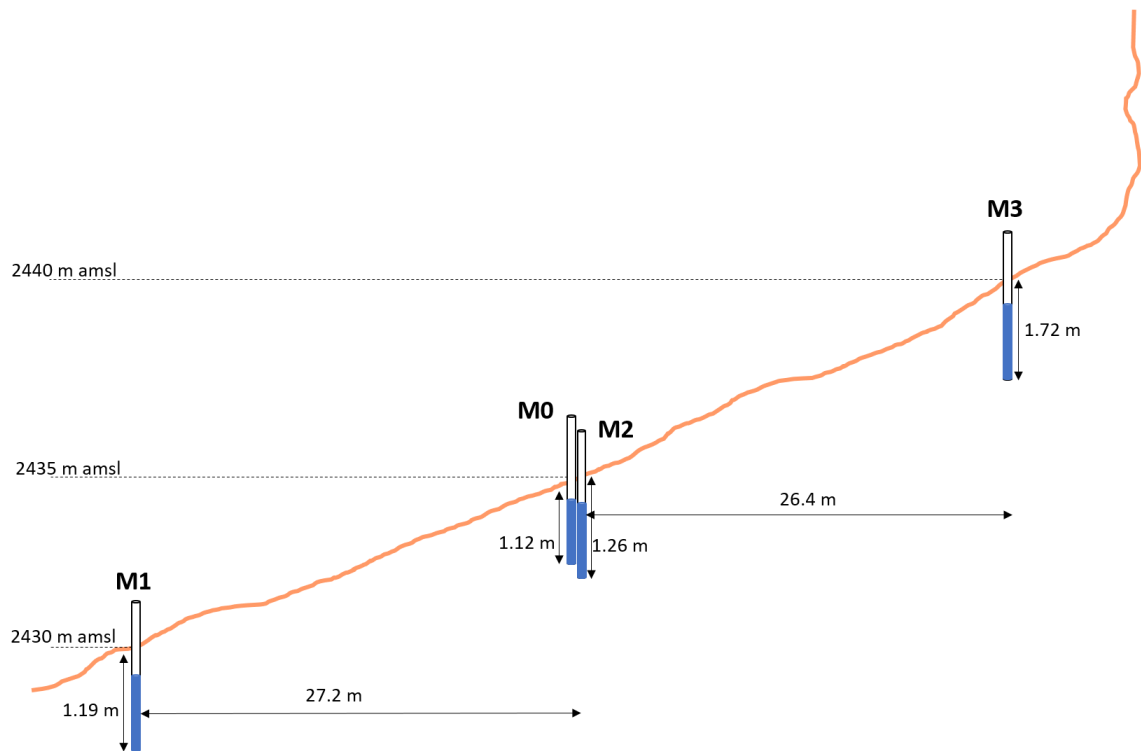


Figure B.1: Schematic of groundwater level in piezometers on moved slope. M0 and M2 are actually located behind each other, perpendicular to M1-M3

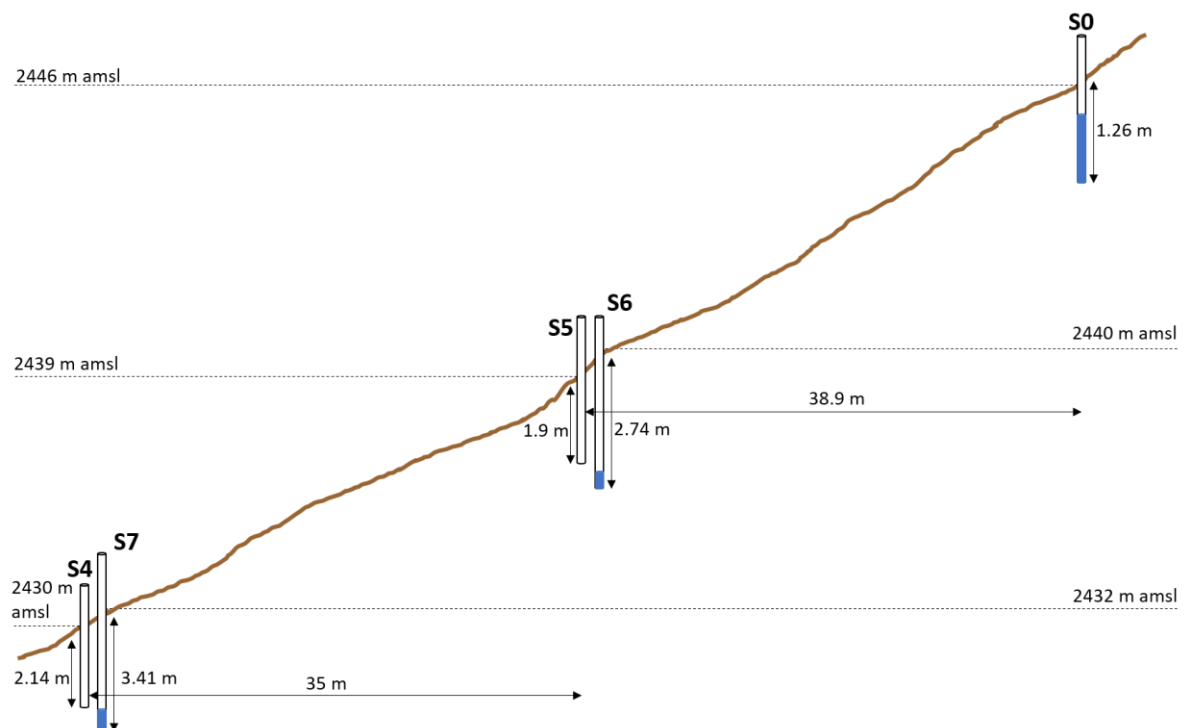


Figure B.2: Schematic of groundwater level in piezometers on stable slope S1. S6 and S7 are installed next to S5 and S4 resp. at a later date (and greater depth).

## Appendix C - Hydraulic conductivity and infiltration calculations

Formula C.1 is used to calculate the  $K_{sat}$  value from in-situ auger hole tests.

$$K_{Sat} = 1.15r \frac{\log\left(h_0 + \frac{1}{2}r\right) - \log\left(h_t + \frac{1}{2}r\right)}{t - t_0} \quad (C.1)$$

$r$  = auger hole radius (m)

$h_0$  = water depth in auger hole at time  $t_0$  (m)

$h_t$  = water depth in auger hole at time  $t$  (m)

$t - t_0$  = difference in time step between start and end of test

For manual measurements the depth from the top of the hole to the water level was subtracted from the total depth of the hole to calculate the water depth. Continuous measurements using a pressure devices required translating pressure to water depth. In both cases usually only the last part of the test was used, when the infiltration rate had become more or less constant, to ensure the soil was truly saturated.

Formula C.2 shows the equation used to calculate  $K_{sat}$  from laboratory constant head tests.

$$K_{Sat} = \frac{Q}{A} \frac{dz}{dh} \quad (C.2)$$

$A$  (cm<sup>2</sup>) is the area of the sample in contact with water.  $Q$  (cm/min) is the amount of water that has passed through the sample (able to read of the gauge of the Mariotte bottle).  $Dz$  (cm) is the height of the sample ring and  $dh$  (cm) is the drop in water height in Mariotte bottle.

Figure C.1 shows typical values of permeability for different textures (De Smedt, 2013)

Texture	k (m/s)
Coarse gravel	> 0.1
Medium gravel	0.01 – 0.1
Fine gravel	$10^{-3}$ – $10^{-2}$
Coarse sand	$10^{-4}$ – $10^{-3}$
Medium sand	$10^{-5}$ – $10^{-4}$
Fine sand	$10^{-6}$ – $10^{-5}$
Coarse silt	$10^{-7}$ – $10^{-6}$
Medium silt	$10^{-8}$ – $10^{-7}$
Fine silt	$10^{-9}$ – $10^{-8}$
Clay	< $10^{-9}$

Figure C.1: Typical ranges of the permeability for different soil textures

Philip's (1957) equation from Cammeraat et al. (2001).

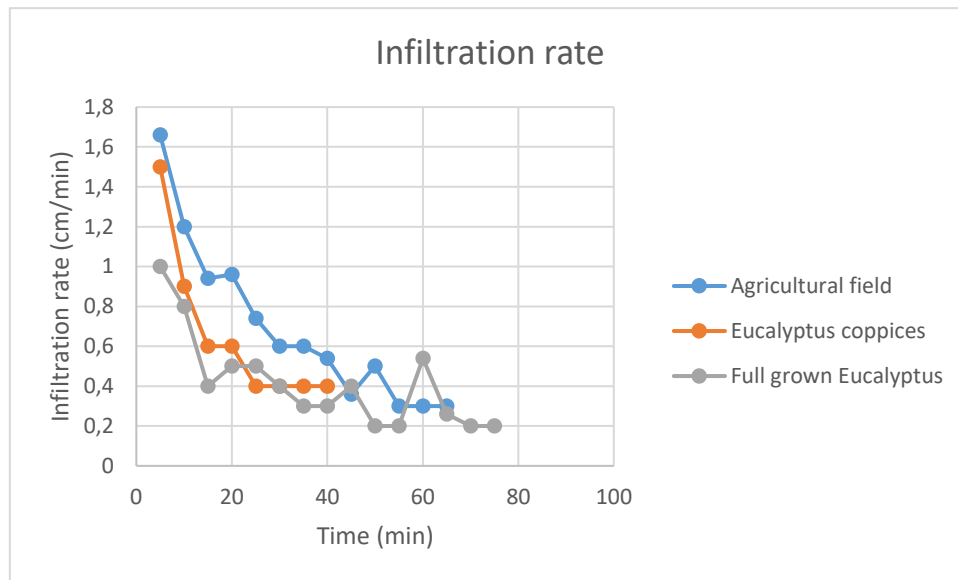
$$f = \frac{S}{2\sqrt{t}} + A \quad (C.3)$$

$f$  is the infiltration rate ( $L \cdot T^{-1}$ ),  $S$  represents the diffusivity ( $L \cdot T^{-1/2}$ ), and  $A$  ( $L \cdot T^{-1}$ ) is a gravity term and related to the hydraulic conductivity through:

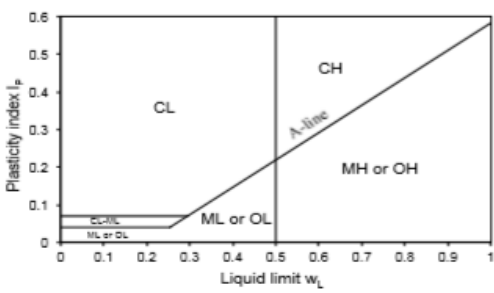
$$K = \frac{A}{M} \quad (C.4)$$

Where  $M$  is a parameter between  $1/3 - 2/3$  provided that the time of infiltration is not too large, and  $S$  is small enough (not very dry soils). Hence, using Philip's equation does not give a good estimate for  $K$  because  $S$  was too large (i.e. the soil could have been too dry).

Another way to roughly estimate the hydraulic conductivity is through the field capacity of the infiltration test. This is the maximum amount of water a soil can accommodate after a longer period of infiltration. Figure C.2 shows a constant infiltration rate, indicating field capacity has been reached, around 0.3cm/min or 5E-5 m/s, which corresponds to a hydraulic conductivity of medium sand.



# Appendix D – Unified Soil Classification System (from De Smedt (2013))

Texture	Main property	Symbol	Description	Fine fraction	Particle distribution	Plasticity	Remarks
Coarse-grained soil  > 50% is retained by sieve n° 200	Gravel  > 50% of the coarse fraction is retained by sieve n° 4	GW	Well graded gravel	< 5%	$C_u > 4$ and $1 < C_c < 3$		Double symbols are used if: (1) the fine fraction is between 5 and 12% (for example GP-GM), or (2) the soil plots above the A-line and $I_p$ is between 0.04 and 0.07 (for example GC-GM).
		GP	Poorly graded gravel	< 5%	Not as above		
		GM	Silty gravel	> 12%		Below the A-line or $I_p < 0.04$	
		GC	Clayey gravel	> 12%		Above the A-line and $I_p > 0.07$	
	Sand  < 50% of the coarse fraction is retained by sieve n° 4	SW	Well graded sand	< 5%	$C_u > 6$ and $1 < C_c < 3$		
		SP	Poorly graded sand	< 5%	Not as above		
		SM	Silty sand	> 12%		Below the A-line or $I_p < 0.04$	
		SC	Clayey sand	> 12%		Above the A-line and $I_p > 0.07$	
Fine-grained soil  < 50% is retained by sieve n° 200	Low plasticity  $w_L < 0.5$	ML	Low plastic silt	<p>The classification is based on the plasticity chart of Casagrande.</p>  <p>The symbol O (organic soil) is used when the liquid limit decreases by more than 25% after oven drying.</p>			
		CL	Low plastic clay				
		OL	Low plastic organic soil				
	High plasticity  $w_L > 0.5$	MH	High plastic silt				
		CH	High plastic clay				
		OH	High plastic organic soil				
Organic		Pt	Peat	Visual observation			

## Appendix E – Atterberg limits results for Karago landslide

Samples label	Soil depth (m)	Soil water W (%)	Plastic limit (PL) %	Shrinkage limit SL) %	Liquid limit LL %	Plasticity index (PI)	Consistency index (CI)	Classification based on PI	Classification based on CI
ML1	0-480	21	21	21	31	10	3.1	Medium plasticity	Very soft soil
ML2	480-550	27	34	24	39	5	7.8	Low plasticity	Very soft soil
ML3	550-610	32	34	22	43	9	4.8	Low plasticity	Very soft soil
ML4	610-690	39	34	21	38	4	9.5	Slightly plastic	Very soft soil
ML5	>690	45	31	19	36	5	7.2	Low plasticity	Very soft soil
S0L1	0-15	42	56	25	69	13	5.3	Medium plasticity	Very soft soil
S0L2	15-65	18	34	22	37	3	12.3	Slightly plastic	Very soft soil
S0L3	65-175	32		19					To be repeated
S0L4	>175	13	28	17	30	2	15.0	Slightly plastic	Very soft soil
S1L1	0-95	33	47	24	62	15	4.1	Medium plasticity	Very soft soil
S1L2	95-165	14	29	19	32	3	10.7	Slightly plastic	Very soft soil
S1L3	165-240	19	32	23	36	4	9.0	Slightly plastic	Very soft soil

## Appendix F – Screenshots of SLIP5EX spreadsheet

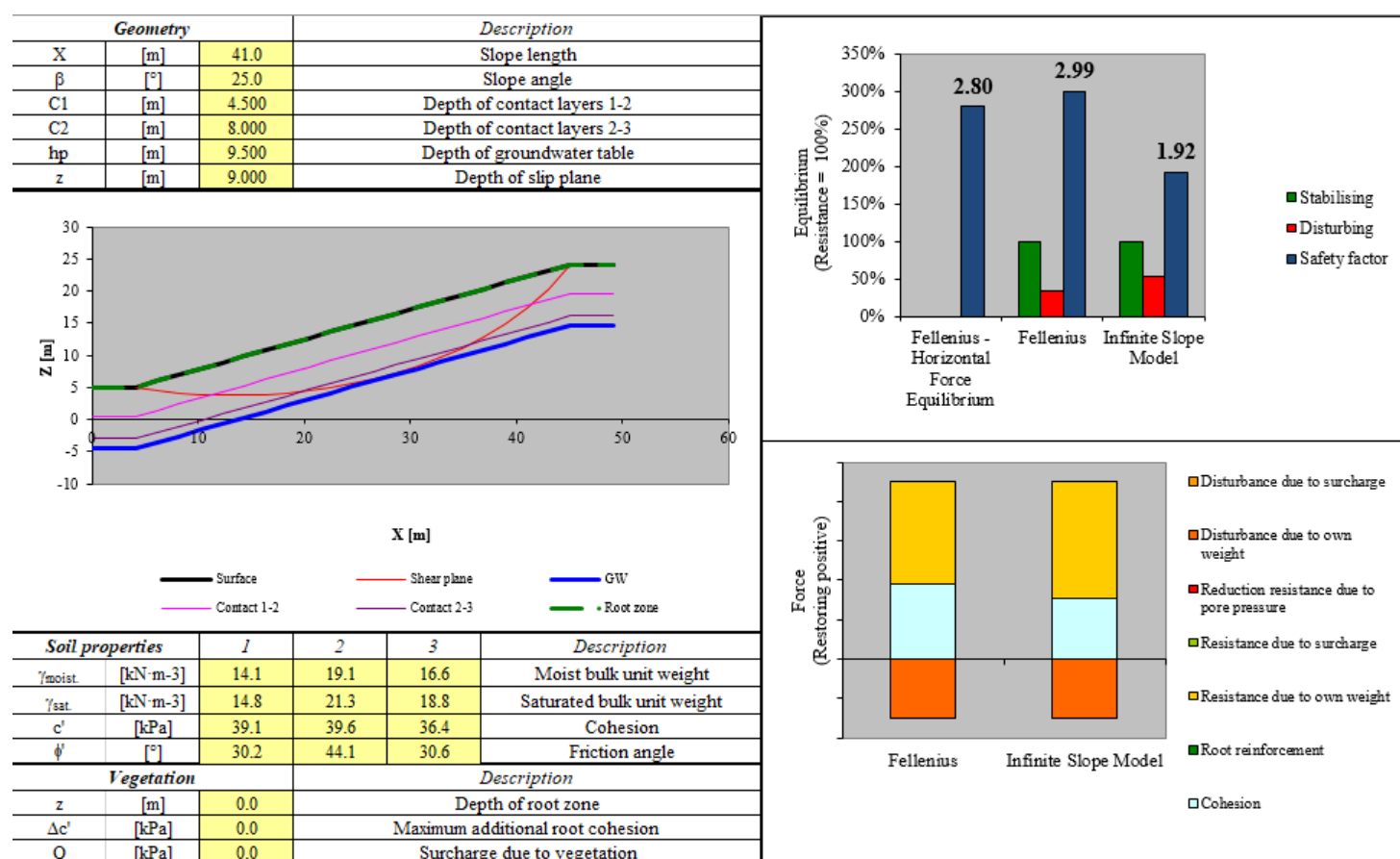


Figure C.1: Screenshot of a SLIP5EX run of landslide nr. 50, with C and  $\phi$  values from the direct shear results.



Appendix G – Literature values for  $C$  and  $\phi$ , and typical bulk unit weight for different soil types

Soil type	Friction angle $\phi^\circ$	Cohesion $c'$ (kPa)
Peat	$< 15^\circ$	2 - 10
Clay		
Soft	$< 17.5^\circ$	$< 10$
Medium hard	$17.5 - 22.5^\circ$	10 - 25
Hard	$> 22.5^\circ$	$> 25$
Silt		
Soft	$< 27.5^\circ$	$< 2$
Medium hard	$27.5 - 32.5^\circ$	2 - 10
Hard	$> 32.5^\circ$	$> 10$
Sand or gravel		0
Very loose	$< 30^\circ$	
Loose	$30^\circ - 32.5^\circ$	
Medium dense	$32.5^\circ - 35^\circ$	
Dense	$35^\circ - 37.5^\circ$	
Very dense	$> 37.5^\circ$	

Figure E.1: Typical values for friction angle and cohesion depending on soil type (De Smedt, 2013)

Soil type	$\gamma_s$ (kN/m <sup>3</sup> )	$\gamma_{dry}$ (kN/m <sup>3</sup> )	$\gamma_{sat}$ (kN/m <sup>3</sup> )
Gravel	26.5	16 - 19	20 - 23
Sand	26.5	14 - 19	18 - 22
Silt	26.5	14 - 19	18 - 21
Clay - soft	26 - 28	9 - 14	14 - 17
Clay - medium	26 - 28	16 - 18	17 - 21
Clay - hard	26 - 28	17 - 18	21 - 24
Peat	10 - 12	1 - 7	10 - 14

Figure E.1: Typical values of unit weight depending on soil type (De Smedt, 2013).

## Appendix H – Landslide catalogue

The data in *italics* was collected during the field visit. The other data was already collected in a prior landslide inventory.

Landslide 50	
Date of visit	15-9-2018
Remarks	<i>V shaped. The inner point of the V was due to sliding. From the sides of the V people had been taking soil to make bricks. Layer thickness was difficult to determine since it was not the same on both sides of the V. So differences of up to 2m for the bottom layer were observed. Also one side, more often in the sun, clearly had harder soil, though it was the same type on both sides.</i>
Number	50
District	Nyabihu
Sector	Karago
Village	
Location	S 01 38 46.7, E 029 28 36.7
Date of sliding	1-5-1998
L (m)	41
W (m)	32
D (m)	9
Slope (degrees)	8-17
Shape	<i>Straight</i>
Movement type	Rotational
Lithology	Pegmatite
Landuse	Forestry
Possible cause	<i>Brick making</i>
Layer 1	<i>brown/black; organic; loose; many roots; 10.8% VWC; 0-3.5m</i>
Layer 2	<i>Light brown; sandy/organic; loose, dry soil; some roots; too hard for VWC measurement; 3.5-4.5m</i>
Layer 3	<i>Reddish with some brown; clay with minerals &amp; small gravels; outside soft, inside hard-very hard (depending on side); no roots; compact; 4.5-8m</i>
Layer 4	<i>Slip surface: white/yellow with black sand; compact but easy to dig; no roots; 18.5% VWC; &gt;8m</i>

Landslide 63	
Date of visit	15-08-2018
Remarks	<i>Main study site. One moved and two stable slopes.</i>
Number	63
District	Nyabihu
Sector	Karago
Village	<i>Bukongora</i>
Location	S1°39'3.3, E29°30'30.7
Date of sliding	1-3-2016
L (m)	50
W (m)	15
D (m)	8
Slope (degrees)	32-45
Shape	<i>Straight</i>
Movement type	Rotational
Lithology	Pegmatite
Landuse	Forestry
Possible cause	Road cutting
Layer 1	<i>Light colored; clayey soil desposited for construction; no roots; compact; 20.6% VWC; 0-4.80m</i>
Layer 2	<i>Light colored clay; no roots; very hard; 18.6% VWC; 4.8-5.5m</i>
Layer 3	<i>Yellowish sand; no roots; very hard; 16.4% VWC; 5.5-6.1m</i>
Layer 4	<i>Light colored clay; no roots; hard; 21.3% VWC; 6.1-6.9m</i>
Layer 5	<i>Light colored clay; no roots; softish; wet; 33% VWC; &gt;6.9m</i>

<b>Landslide 128</b>	
Date of visit	12-9-2018
Remarks	Landslide from April 2018
Number	128
District	Nyabihu
Sector	Muringa
Village	
Location	S 01 44 40.8, E 029 30 46.6
Date of sliding	28-4-2018
L (m)	35
W (m)	44
D (m)	16
Slope (degrees)	32-45
Shape	Ellipsoid/Straight
Movement type	Rotational
Lithology	Pegmatite
Landuse	Agriculture
Possible cause	Heavy rain
Layer 1	Slip surface?: Dark brown, organic-ish; small roots present; loose, soft; 20.3% VWC; 0-9m
Layer 2	Light colored; no roots; hard, very compact quartz/gravel; >9m

<b>Landslide 187</b>	
Date of visit	13-9-2018
Remarks	Very steep. Up slope of the road. Rains have made the soil to continue moving down slowly (according to locals)
Number	187
District	Nyabihu
Sector	Jomba
Village	
Location	S 01 41 10.1, E 029 31 21.2
Date of sliding	28-4-2018
L (m)	7
W (m)	5
D (m)	4
Slope (degrees)	8-17
Shape	Straight
Movement type	Rotational
Lithology	Pegmatite
Landuse	Forestry
Possible cause	Deforestation / erosion by rainfall
Layer 1	Light brown, beige; roots present; dry, somewhat hard, loose and crumbling soil. 7% VWC; 0-2.7m
Layer 2	Beige, orange color; no roots; hard; silty with some gravel; 2.7-3.8m
Layer 3	Slip surface: more orange; no roots; softer but still hard; more clay, less gravel; 15.4% VWC; >3.8m

<b>Landslide 219</b>	
<b>Date of visit</b>	13-9-2018
<b>Remarks</b>	<i>Steep slope sliding into a (deep) terrace drain. Seemed to have slid in parts so ambiguous if depth is total length or half the length. Failure mechanism unsure, could possibly be due to toe erosion by the drain. Also made slip surface identification difficult.</i>
<b>Number</b>	219
<b>District</b>	Nyabihu
<b>Sector</b>	Rambura
<b>Village</b>	
<b>Location</b>	S 01 40 06.8, E 029 31 35.6
<b>Date of sliding</b>	26-4-2017
<b>L (m)</b>	10
<b>W (m)</b>	6
<b>D (m)</b>	2
<b>Slope (degrees)</b>	17-25
<b>Shape</b>	<i>Straight</i>
<b>Movement type</b>	Rotational
<b>Lithology</b>	Pegmatite
<b>Landuse</b>	Agricultural
<b>Possible cause</b>	<i>Agricultural practices / toe erosion of terrace drain</i>
<b>Layer 1</b>	<i>Light brown; silty organic; roots present; medium hard; 20.5% VWC; 0-1.3m</i>
<b>Layer 2</b>	<i>Slip surface?: Dark brown/grey with orange tints; clayey with some gravel; softish; no roots; 24% VWC; 1.3-5.5m</i>
<b>Layer 3</b>	<i>Slip surface?: Very orange with brown; oxidized clay and weather minerals; soft; no roots; 26.4% VWC; 5.5-6.5m Possibly same material as layer above but more saturated, and having slid at a different time.</i>
<b>Layer 4</b>	<i>White/light colored; soft; sand with mineral deposits; no roots; 24.6% VWC; &gt;6.5m</i>

## Appendix I – Direct shear results moved slope M (layer 5)

Layer	Depth (m)	Notes	Assumed density (kN/m <sup>3</sup> )	Height of soil above (m)	Pressure (kN/m <sup>2</sup> )	Load (kg/36cm <sup>2</sup> )	Loads applied (kg)	Pressures applied (kPa)	Shear speed (mm/hr)
1	0-4.80	Deposited soil due to construction activities	16	4.8	76.8	27.648	20, 40, 60 kg	55, 110, 165 kPa	2,1,1 mm/hr
2	4.80-5.50	Very hard clay	18	5.5	89.4	32.184	20, 40, 60 kg	55, 110, 165 kPa	1,1,1 mm/hr
3	5.50-6.10	Very hard sand (yellow color)	20	6.1	101.4	36.504	30, 50, 80 kg	85, 140, 225 kPa	2,2,2 mm/hr
4	6.10-6.90	Hard clay	18	6.9	115.8	41.688	30, 50, 80 kg	85, 140, 225 kPa	1,1,1 mm/hr
5	>6.90	<b>Clay (softish) with water table</b>	<b>20</b>	<b>8</b>	<b>137.8</b>	<b>49.608</b>	<b>40, 60, 100 kg</b>	<b>110, 165, 275 kPa</b>	<b>1,1,1 mm/hr</b>

Table I.1. Table with basic calculations to calculate the loads applied and shear speed of the soil layers of the moved slope

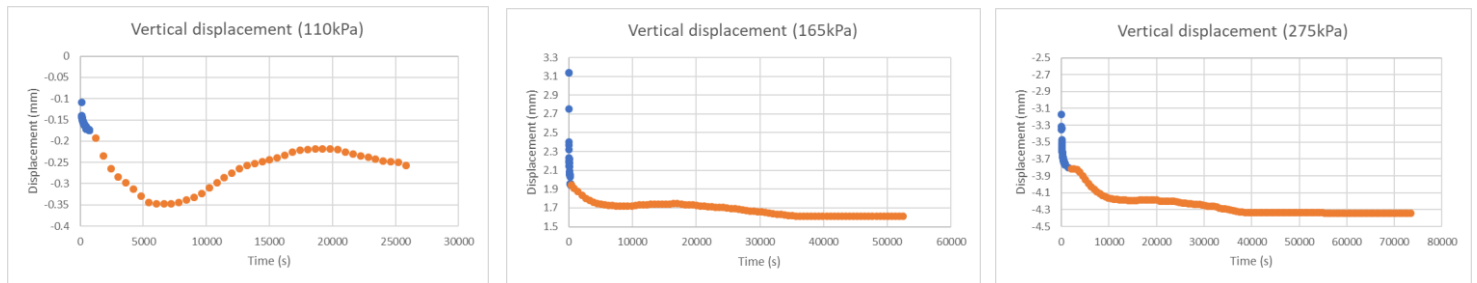


Figure I.1: Vertical displacements for the 3 tests of ML5. Blue is consolidation prior to shearing. Orange is vertical displacement during shearing.

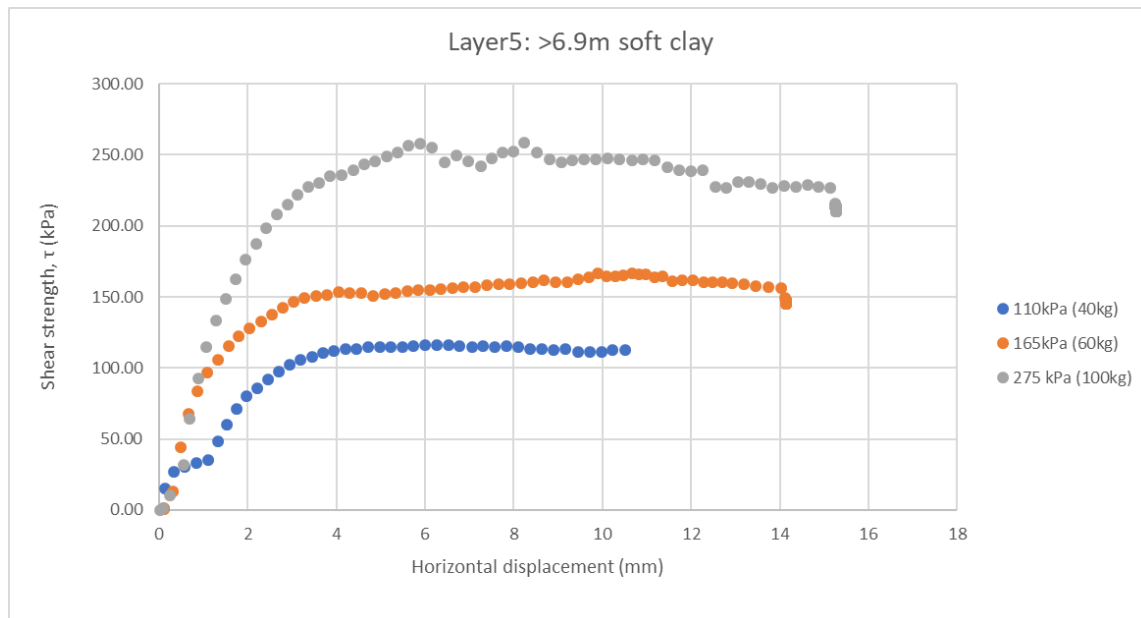


Figure I.2: Raw results of the 3 direct shear tests for different normal loads.

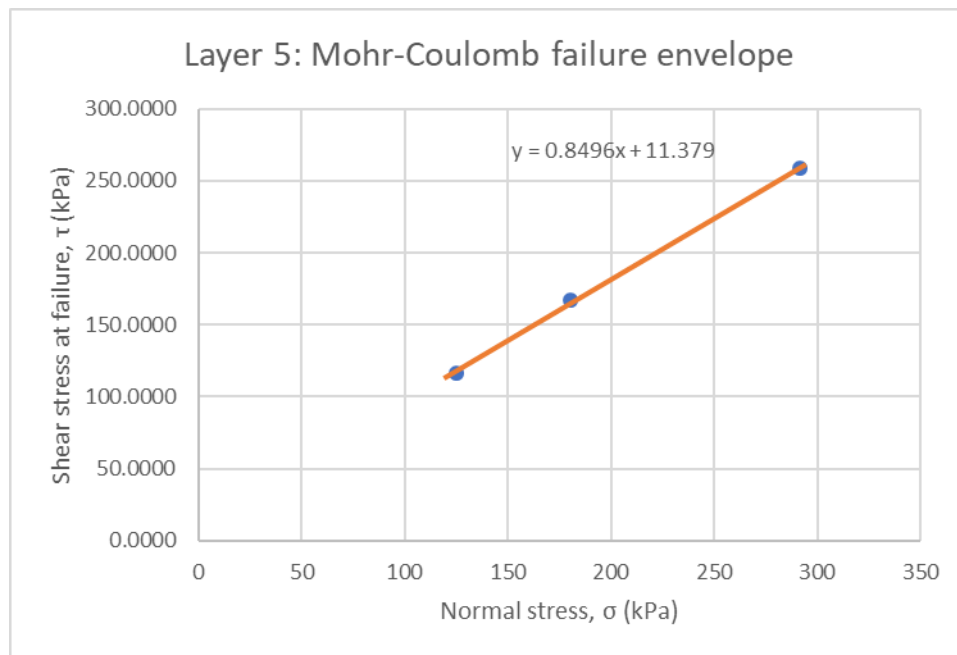


Figure I.3: Mohr-Coulomb failure envelope of the 5<sup>th</sup> layer of the moved slope. Y-intercept of best fit line is the cohesion. The slope of the best fit line is the angle of internal friction.